AD_____

Award Number: DAMD17-01-1-0023

TITLE: A Novel Prostate Epithelium-Specific Transcription Factor in Prostate Cancer

PRINCIPAL INVESTIGATOR: Towia A. Libermann, Ph.D.

CONTRACTING ORGANIZATION: Beth Israel Deaconess Medical Center
Boston, Massachusetts 02215

REPORT DATE: June 2004

TYPE OF REPORT: Final

PREPARED FOR: U.S. Army Medical Research and Materiel Command
Fort Detrick, Maryland 21702-5012

DISTRIBUTION STATEMENT: Approved for Public Release;
Distribution Unlimited

The views, opinions and/or findings contained in this report are those of the author(s) and should not be construed as an official Department of the Army position, policy or decision unless so designated by other documentation.

20050105 077

REPORT DOCUMENTATION PAGE

Form Approved
OMB No. 074-0188

Public reporting burden for this collection of information is estimated to average 1 hour per response, including the time for reviewing instructions, searching existing data sources, gathering and maintaining the data needed, and completing and reviewing this collection of information. Send comments regarding this burden estimate or any other aspect of this collection of information, including suggestions for reducing this burden to Washington Headquarters Services, Directorate for Information Operations and Reports, 1215 Jefferson Davis Highway, Suite 1204, Arlington, VA 22202-4302, and to the Office of Management and Budget, Paperwork Reduction Project (0704-0188), Washington, DC 20503

1. AGENCY USE ONLY (Leave blank)

2. REPORT DATE
June 2004

3. REPORT TYPE AND DATES COVERED
Final (1 Jun 01-31 May 04)

4. TITLE AND SUBTITLE
A Novel Prostate Epithelium-Specific Transcription Factor in Prostate Cancer

5. FUNDING NUMBERS
DAMD17-01-1-0023

6. AUTHOR(S)
Towia A. Libermann, Ph.D.

7. PERFORMING ORGANIZATION NAME(S) AND ADDRESS(ES)
Beth Israel Deaconess Medical Center
Boston, Massachusetts 02215

E-Mail: tliberma@bidmc.harvard.edu

8. PERFORMING ORGANIZATION REPORT NUMBER

9. SPONSORING / MONITORING AGENCY NAME(S) AND ADDRESS(ES)
U.S. Army Medical Research and Materiel Command
Fort Detrick, Maryland 21702-5012

10. SPONSORING / MONITORING AGENCY REPORT NUMBER

11. SUPPLEMENTARY NOTES

12a. DISTRIBUTION / AVAILABILITY STATEMENT
Approved for Public Release; Distribution Unlimited

12b. DISTRIBUTION CODE

13. ABSTRACT (Maximum 200 Words)

Prostate cancer has become the most common solid cancer in older men and is one of the most frequent causes of cancer deaths. The poor prognosis for advanced prostate cancer reflects in part the lack of knowledge about the tumor's basic biology. Our goal is to understand the role of a novel prostate-specific transcription factor, PDEF, a member of an oncogene family in human prostate cancer. Expression of this factor is significantly elevated in cancerous portions of the prostate. PDEF appears to be involved in regulating expression of the diagnostic prostate cancer marker PSA and cooperates with the androgen receptor. Thus, our hypothesis is that PDEF contributes to the progression from an initially hormone-dependent prostate cancer to a hormone-independent cancer. We propose to determine the role of this novel gene in prostate cancer using , cell culture models, animal models and patient samples of prostate cancer.

Our results strongly suggest that PDEF plays a critical role in prostate cancer formation or progression. Our long term goal is to explore the possibility to use this new factor as another diagnostic tool and as a potential therapeutic target for prostate cancer.

14. SUBJECT TERMS
Prostate Cancer, PDEF, Transcription Factor, Migration, Invasion, EMT

15. NUMBER OF PAGES
34

16. PRICE CODE

17. SECURITY CLASSIFICATION OF REPORT	18. SECURITY CLASSIFICATION OF THIS PAGE	19. SECURITY CLASSIFICATION OF ABSTRACT	20. LIMITATION OF ABSTRACT
Unclassified	Unclassified	Unclassified	Unlimited

Table of Contents

Cover..... 1

SF 298..... 2

Table of Contents..... 3

Introduction..... 4

Body..... 4-14

Key Research Accomplishments..... 14

Reportable Outcomes..... 14-15

Conclusions..... 15

References..... 15

Appendices..... 16

List of Personnel.....

Appended Publication.....

a. Introduction

Prostate cancer has become the most common solid cancer in older men and is one of the most frequent causes of cancer deaths. Although androgen ablation therapy, surgery and radiation therapy are effective for the treatment of local prostate cancer, there is no effective treatment available for patients with metastatic androgen-independent disease. The poor prognosis for androgen-independent advanced prostate cancer reflects in part the lack of knowledge about the tumor's basic biology, although progress has been made in identifying defects of various oncogenes and tumor suppressor genes. In particular, very little is known about the molecular mechanisms that trigger the conversion of an initially androgen-dependent cancer to androgen-independence. Our goal was to understand the role of a novel prostate epithelium-specific transcription factor, PDEF, a member of the Ets transcription factor/oncogene family in human prostate cancer that uniquely among the Ets family prefers binding to a GGAT rather than a GGAA core. PDEF is expressed in the luminal epithelial cells of normal human prostate and PDEF expression is significantly elevated in cancerous portions of the prostate. PDEF acts as an androgen-independent transcriptional activator of the PSA promoter, a diagnostic marker used for monitoring androgen-dependent and –independent prostate cancer. PDEF also directly interacts with the DNA binding domain of the androgen receptor and with the prostate-specific homeobox gene NKX3.1 and enhances androgen-mediated activation of the PSA promoter. Thus, our hypothesis was that PDEF bypasses or activates the androgen receptor and thereby contributes to the progression from an initially androgen-dependent prostate cancer to an androgen-independent cancer. We proposed to determine the role of this novel member of the Ets family in the conversion of prostate cancer to androgen independence. Our results as well as the critical roles of other Ets factors in cellular differentiation and tumorigenesis strongly suggested that PDEF is an important regulator of prostate gland development and plays a role in prostate epithelial cell transformation and/or prostate cancer progression. Our long term goal was to explore the possibility to use this new factor as another diagnostic tool and as a potential therapeutic target for prostate cancer. Thus, our original specific aims were as follows:

Specific Aim #1. Does PDEF play a crucial role in prostate cancer development or progression?

A) What is the effect of overexpressing wild type or dominant-negative PDEF expression on prostate epithelial cells in transgenic mice?

B) Can inhibition of PDEF function interfere with LNCaP prostate cancer cell transformation, invasion, or proliferation, or androgen dependence?

C) Does forced PDEF overexpression in PDEF negative primary human prostate epithelial cells affect prostate epithelial cell differentiation, transformation, invasion, proliferation, or androgen independence?

Specific Aim #2. What are the target genes in prostate cancer cells regulated by PDEF?

A) Use cDNA and oligonucleotide microarrays to identify PDEF target genes in primary prostate epithelial cells and LNCaP prostate cancer cells.

B) Use bioinformatics tools to cluster PDEF target genes and to define biological pathways for PDEF.

C) Determine whether PDEF is a direct regulator of identified target genes by analyzing the ability of PDEF to bind to and transactivate promoter/enhancer regions of PDEF target genes.

Specific Aim #3. Can PDEF be used as a diagnostic or prognostic marker for prostate cancer?

A) Is PDEF over- or under-expressed in benign prostate hyperplasia, prostate intraepithelial neoplasia (PIN), and/or in advanced prostate cancer?

b. Body

Most of the specific aims outlined originally were accomplished. We made significant progress in all our aims and were able to provide new insights into the role and function of

PDEF in prostate cancer. Our data for a large part confirmed our original hypothesis, but also added various surprising and unexpected features of PDEF. We are now in the process to incorporate the results of our studies into a series of three mansucripts. Two other manuscripts funded by this grant have been published already. Following is a summary of the progress made during the funding period.

1. Chromosomal mapping and genomic organization of the human PDEF gene and identification of a functional promoter

We reported the chromosomal mapping, the structural organization and identification of a functional promoter of the human PDEF gene. The human PDEF gene is positioned within the MHC cluster region on chromosome 6p21.3 and contains 6 exons, which span approximately 18.5kb of genomic DNA. Analysis of the immediate promoter region of the human PDEF genes demonstrates the presence of a TATA box as well as potential binding sites for Ets factors, AP-1, and an androgen response element. Transfection experiments demonstrated that a 2.5 kb fragment of the 5' upstream region acts as a strong promoter only in breast and prostate epithelial cell lines.

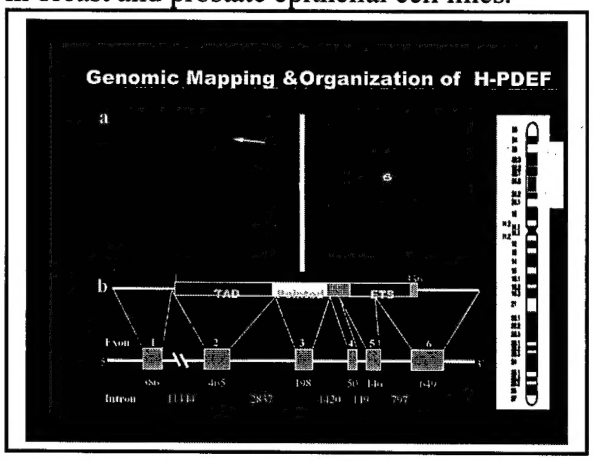

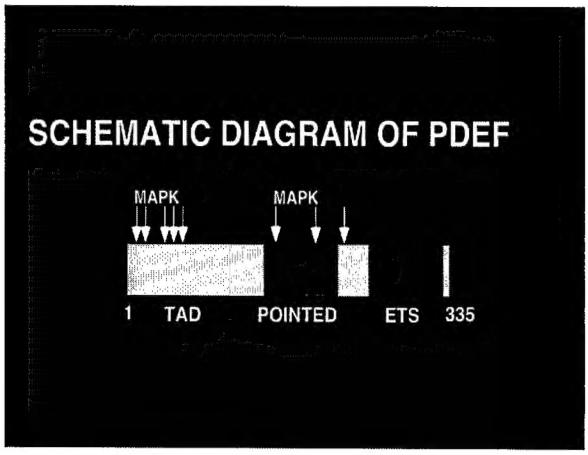

2. Dominant-negative PDEF mutant specifically inhibits PDEF mediated transactivation of the PSA promoter

We have generated a dominant-negative deletion mutant of PDEF that lacks the amino-terminal transactivation domain ($PDEF_{\Delta 1\text{-}141}$). This mutant is still able to bind to PDEF binding sites, but does not transactivate. Increasing amounts of an expression vector for this mutant inhibited transactivation of the PSA promoter by wild type PDEF by more than 90% . These data suggest that this PDEF mutant acts as a specific dominant-negative mutant and we have used this mutant to block the activity of endogenous PDEF.

3. Dominant-negative PDEF mutant specifically inhibits endogenous PSA gene expression in PSA positive LNCaP cells

In order to evaluate whether PDEF is a critical factor for PSA gene expression in vivo we stably transfected PSA positive LNCaP cells with the dominant-negative PDEF mutant, as well as the empty parental expression vector, since LNCaP cells also express endogenous PDEF. Several stably transfected clones were isolated and analyzed by Northern Blotting for expression of the endogenous PSA gene. In contrast to the parental vector control clones that expressed high levels of PSA, clones expressing the dominant-negative PDEF did not express any detectable levels of PSA. These data most vividly demonstrate that PDEF is a critical factor for PSA gene expression and, therefore, may play an important role in prostate cancer.

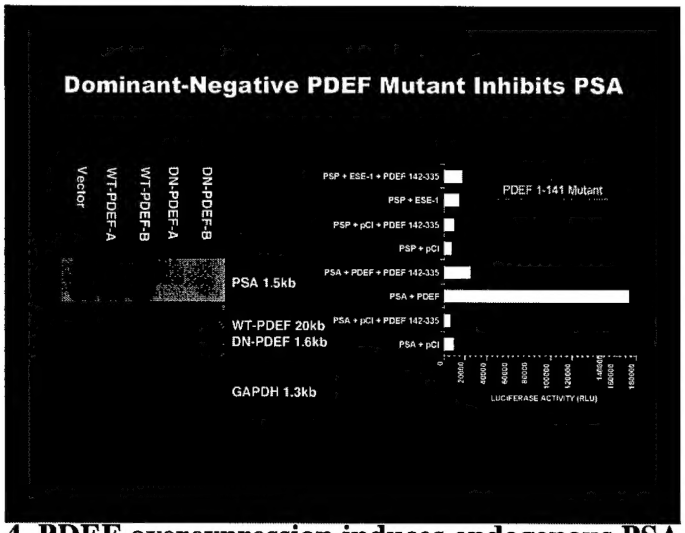

4. PDEF overexpression induces endogenous PSA gene expression in LNCaP cells
We transiently transfected LNCaP cells with an expression vector encoding PDEF to determine whether PDEF overexpression has an effect on endogenous PSA gene expression. Indeed PDEF overexpression significantly enhanced endogenous PSA gene expression in LNCaP cells, confirming the data obtained with the dominant-negative mutant PDEF. Together, all these data place PDEF in the center of PSA gene regulation and may suggest that PDEF plays a role in androgen-independent PSA gene expression in hormone-refractory prostate cancer.

5. PDEF expression is enhanced in human CaP. To determine PDEF expression in CaP, we performed in situ hybridization and immunohistochemistry of primary CaP tissues. Transformed epithelial cells stained strongly for PDEF mRNA and protein, whereas only weak staining was observed in normal prostate epithelium. Tumor tissue did not stain uniformly, but showed striking differences in different parts of tumors and in different patient samples. PDEF expression might be a marker for CaP development and/or progression and could be used as a diagnostic or possibly prognostic marker in prostate biopsies. Northern analysis showed that CaP cell lines LNCaP and PC-3 express high levels of PDEF, whereas primary prostate epithelial cells do not.

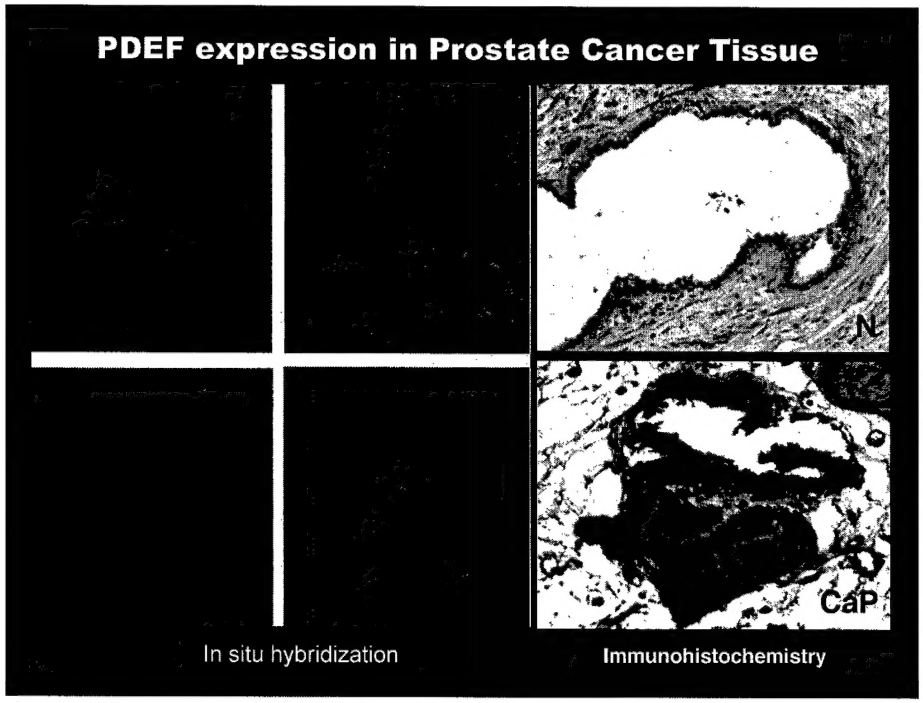

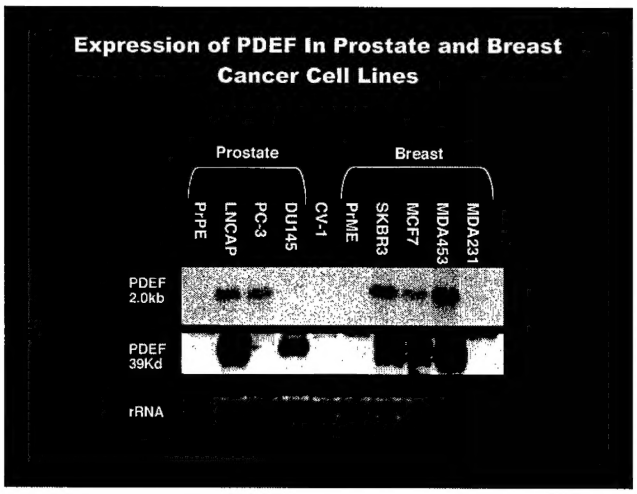

6. Generation of siRNA against PDEF. In order to inhibit endogenous PDEF expression in CaP cells, we have synthesized siRNAs against PDEF. We have tested their efficacy in blocking PDEF expression and the most effective siRNA reduced PDEF protein expression by 80-90% as estimated from Western blot experiments. We have generated in collaboration with Ricardo Correa and Inder Verma lentivirus vectors expressing the PDEF siRNA as well as GFP and we have generated CaP cell lines stably infected with PDEF siRNA.

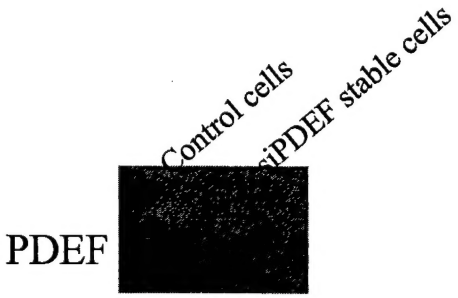

7. Identification of PDEF interacting proteins. Since Ets factors use protein-protein interactions to elicit their biological responses, we are exploring which proteins interact with PDEF. We transfected FLAG tagged PDEF (FLAG-PDEF) into cells for overexpression. PDEF complexed with its interacting proteins was immunoprecipitated using the anti-FLAG antibody and separated by SDS-PAGE. Individual stained bands were digested by trypsin. The trypsin digest was analyzed in a Ciphergen mass spectrometer and a MALDI-TOF/TOF mass spectrometer. We identified several proteins as PDEF interacting proteins including HSP70 and we are now in the process of cloning these proteins into expression vectors for in vitro GST pull down interaction studies.

8. PDEF expression is induced by androgen. Androgen is a critical regulator for CaP growth and PSA expression. Since PDEF is highly expressed in CaP cells and transactivates the PSA promoter, PDEF might be one of the targets for androgen induced prostate growth and transformation. To test this, we measured PDEF transcript levels in response to androgen DHT in LNCaP cells grown in androgen deficient medium. PDEF expression was highly reduced after depletion of androgen and was induced in a dose dependent manner by androgen.

Northern blot analysis of androgen effects on PDEF expression in LNCaP. PDEF transcripts are induced by androgen. (C: charcoal stripped serum, A: androgen DHT, NA: no androgen, N: normal serum).

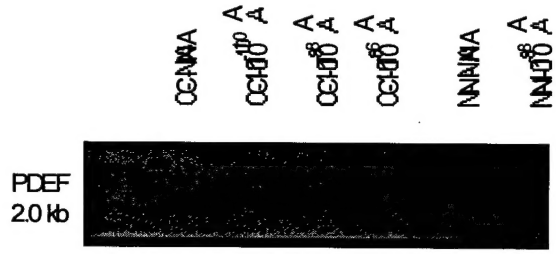

9. TGF-β1 inhibits PDEF expression in CaP. TGF-β family members are one of the few classes of endogenous inhibitors of cell growth. Contrary to the first notion that these proteins may be downregulated in cancer cells to promote their growth, generally there is a marked increase in the expression of TGF-β in many cancers, including those of the prostate. Furthermore, in many of these cancers high expression correlates with more advanced stages of malignancy and decreased survival. The increased expression of TGF-β is usually accompanied by a loss in the growth inhibitory response to TGF-β. Since TGF-β is a major inducer of EMT and inhibition of PDEF induces EMT concomitant with regulation of genes known to be targets for TGF-β, we tested whether PDEF expression is regulated by TGF-β1. TGF-β1 reduced PDEF expression in various CaP cells suggesting that PDEF repression at least partially mediates TGF-β induced EMT.

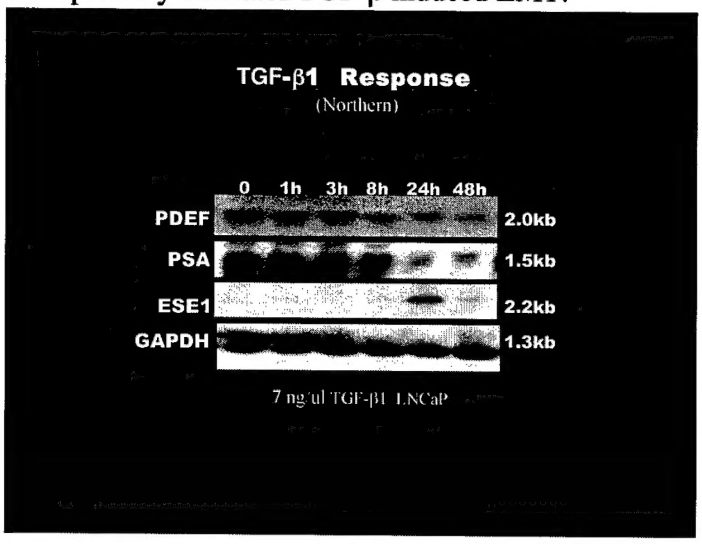

10. PDEF enhances CaP tumor growth in SCID mice. To determine whether PDEF has an effect on tumor formation *in vivo*, we used an orthotopic CaP tumor model in SCID mice. LNCaP cells infected with AdCMVPDEF, AdCMVB-gal or uninfected cells were orthotopically implanted into the prostate of SCID mice. After two month, the animals were examined for tumor formation, tumor weight and PSA expression. Overexpression of PDEF significantly enhanced tumor growth.

11. Inhibition of PDEF expression induces apoptosis and cell cycle arrest of CaP cells. To evaluate the relevance of PDEF for cell survival and cell cycle progression we tested CaP cell lines that stably express the PDEF siRNA by FACS analysis for apoptosis and distribution of cell cycle phases. Inhibition of PDEF expression led to a cell cycle arrest in the S phase resulting in a significant increase in apoptosis.

	G1	G2	S	Apoptosis
LNCaP siGFP	69.6	0	30.3	0.07
LNCaP siPDEF	0	50	50	2.3

12. Treatment of CaP cells with the NSAID Sulindac sulfide induces apoptosis and complete inhibition of PDEF expression. To evaluate whether PDEF might play a role in apoptosis induction by apoptosis inducing anti-cancer drugs we evaluated the effect of sulindac sulfide on PDEF expression and CaP cell survival. Sulindac has recently been demonstrated to inhibit the growth of various types of cancer cells. Real time PCR analysis and transcriptional profiling demonstrated that Sulindac treatment induced a more than 10fold reduction in PDEF expression in PC-3 and DU145 cells. This reduction correlated with apoptosis induction.

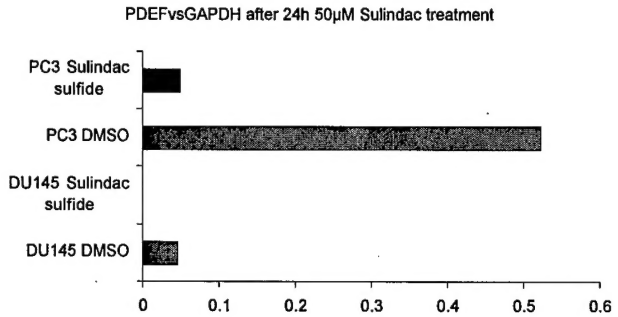

13. PDEF overexpression enhances proliferation and growth of CaP cells in soft agar. Since expression of PDEF was upregulated by androgen and downregulated by TGF-β1, we were interested to know whether PDEF is involved in cell proliferation. We tested LNCaP and PC-3 cells that either overexpress wild type PDEF, dominant negative PDEF or PDEF siRNA in a proliferation assay. PDEF overexpression slightly enhanced the proliferation rate, whereas PDEF siRNA and dominant negative PDEF decreased cell proliferation. Overexpression of PDEF also increased the size of colonies grown in soft agar.

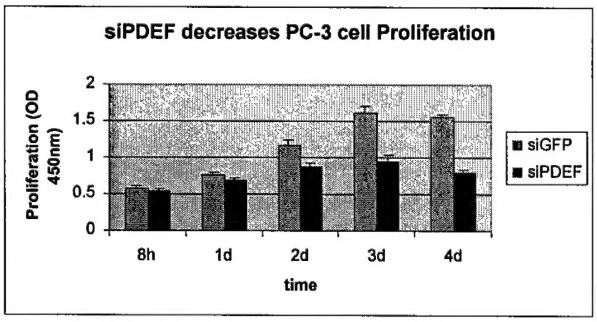

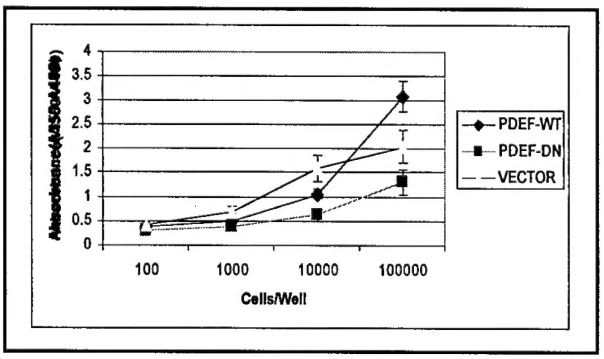

14. PDEF inhibits CaP cell migration and invasion, but enhances adhesion. To evaluate the role of PDEF in cell migration and invasion we tested overexpression of wild type PDEF as well as PDEF siRNA in CaP cell lines. Overexpression of PDEF significantly reduced migration and invasion, whereas inhibition of endogenous PDEF by siRNA strongly enhanced migration and invasion. In contrast to these effects, PDEF overexpression enhanced adhesion, whereas inhibition of endogenous PDEF drastically reduced adhesion.

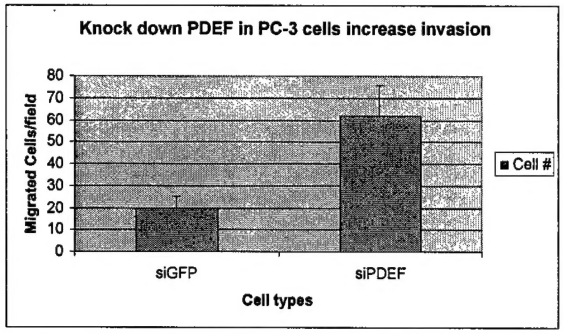

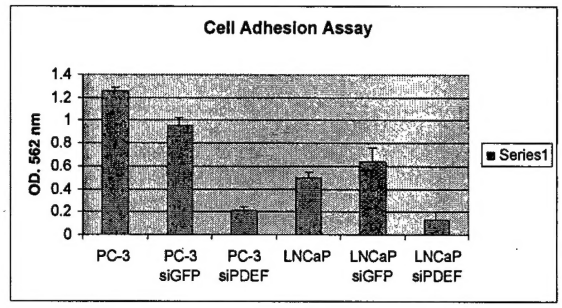

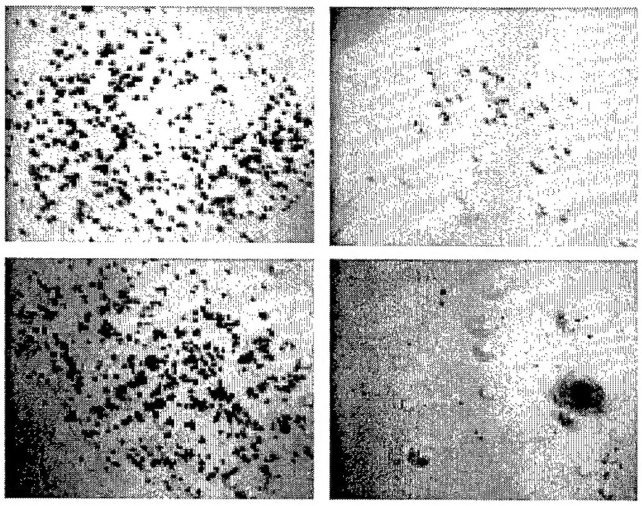

PC-3 siGFP PC-3

PC-3 adhesion after

15. Inhibition of PDEF leads to morphological changes reminiscent of EMT. We evaluated the effect of PDEF on the morphology of CaP cells. Whereas overexpression of PDEF induced a flattening of cells, inhibition of endogenous PDEF changed the morphology of CaP cell lines to a fibroblastoid shape that ressembles EMT.

16. Transcriptional profiling identifies various PDEF target genes involved in adhesion and migration. To determine which genes are targeted by PDEF, we expressed wild type PDEF or PDEF siRNA in LNCaP and PC-3 cells. Different times after infection mRNA was isolated and analyzed by transcriptional profiling on Affymetrix U133A GeneChips. Careful bioinformatics analysis revealed that PDEF enhances or decreases expression of a variety of genes. Particularly interesting were a set of genes that are related to adhesion, migration and invasion including fibronectin, vimentin and E-cadherin. We have validated at least 30 of these targets by real-time PCR. The table below shows a short list of PDEF target genes that are also targeted during EMT and by TGF-β. Using siRNA we demonstrated that genes that are upregulated by PDEF are downregulated by siRNA and genes that are downregulated by overexpression of PDEF become upregulated by siRNA.
In summary, careful analysis of PDEF function and expression has demonstrated that inhibition of PDEF leads to physiological changes that strongly resemble EMT and TGF-β responses.

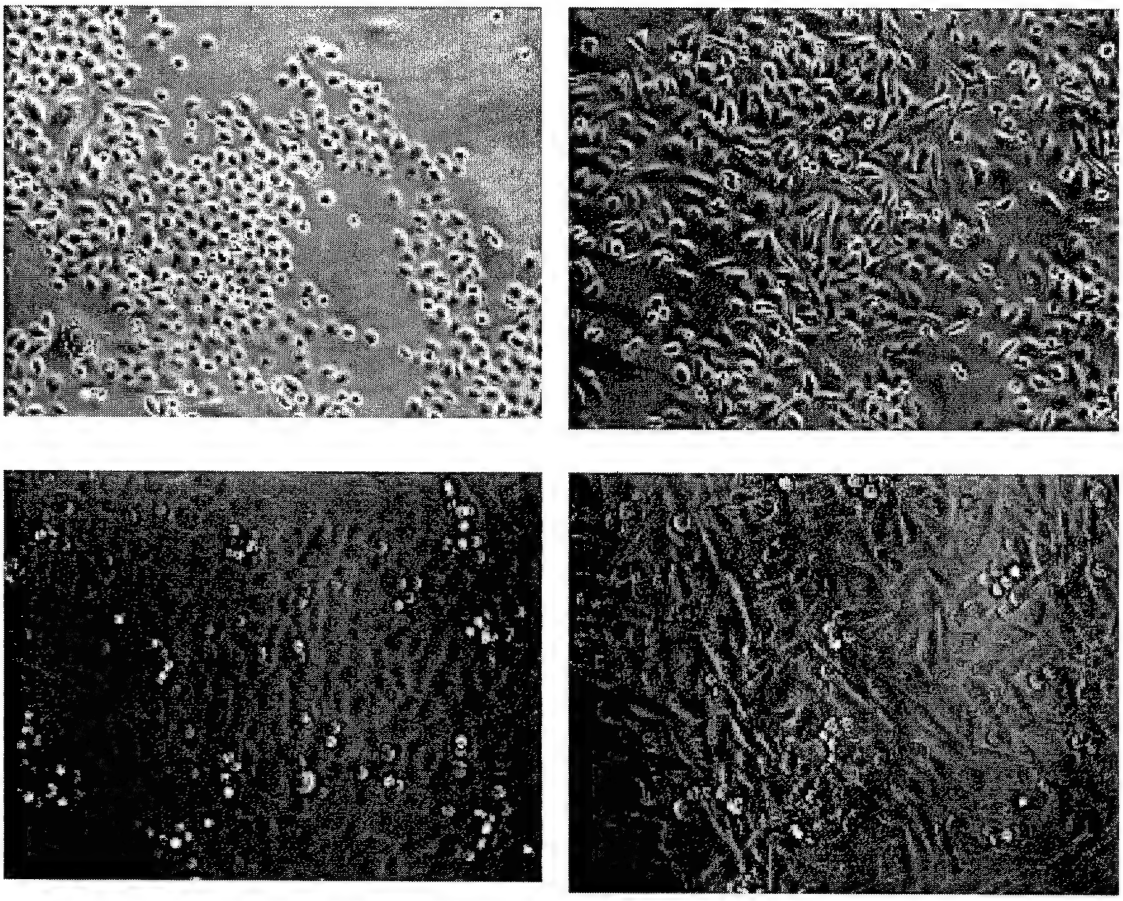

PC-3 siGFP PC-3 siPDEF

PC-3

Acc. No.	Gene name	Fold Change (by siPDEF)
M26251	Vimentin	4
X66405	Collagen, type VI	3
M83218	S100 calcium-binding protein A8	2
U03421	Interleukin-11	2
NM_007287	CD10	3
AJ224869	CXCR4	3
X06115	E-cadherin	-4
M87276	Thrombospondin 1	-4
D50086	Neuropilin	-3
M32745	TGF beta3	-3
M69293	ID-2	-2
BF433902	TNFR11b	-2
NM_001955.1	Endothelin 1	-2
NM_004693.1	K6HF	-2

17. PDEF is a target for Jnk and ERK kinases

The PDEF protein has various putative MAP kinase phosphorylation sites at the amino-terminal transactivation domain. In order to determine whether PDEF may be a target for MAP kinases we performed in vitro kinase assays with FLAG-tagged PDEF and ERK, JNK o rp38 kinases. Both ERK and JNK strongly phosphorylated PDEF indicating that PDEF can indeed be phosphorylated by MAP kinases. To further detail the phosphorylation sites we performed Western blot analysis with anti-phosphothreonine antibodies. This antibody specifically detected PDEF only after phosphorylation by ERK or JNK suggesting that at least some of the phosphorylated residues in PDEF are threonines. We have extended our study to determine whether JNK and ERK can phosphorylate PDEF in vivo and our preliminary data suggest that PDEF indeed gets phosphorylated by these kinases in vivo.

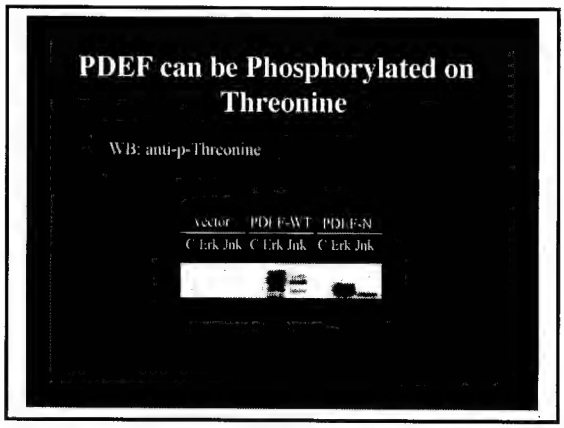

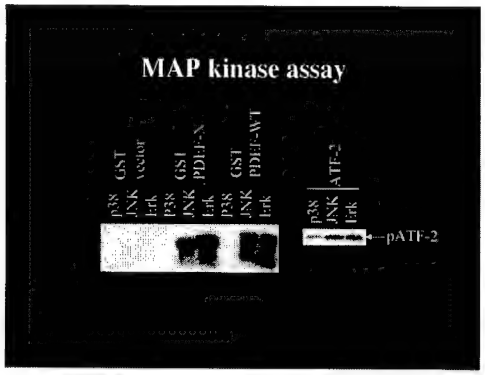

18. Genomic organization of the mouse PDEF gene and generation of knockout constructs

We had previously characterized the human genomic structure of the PDEF gene. We have now sequenced and characterized the murine PDEF gene. The intron/exon structure is very similar to the human gene. We have also sequenced the mouse PDEF promoter sequence and subcloned a 3.1 kb fragment into the luciferase reporter vector. We have started to analyze the activity of the human and mouse PDEF promoter. Most of the activity is present in cells that express endogenous PDEF such as prostate and breast cancer cell lines, whereas PDEF negative cells such as MG-63 osteosarcoma cells and 293 cells express very little PDEF promoter activity. In order to knock out the PDEF gene in mice for studying the effect of PDEF on prostate and mammary gland development, we have generated a construct that deletes the Ets DNA binding domain and the Pointed domain. We have successfully introduced this construct into ES cells and after selection in G418 obtained various neomycin resistant clones. We are now in the process of analyzing these clones by Southern blot hybridization for homologous recombination that deleted the PDEF gene. If successful, we will generate knockout mice within the next few months.

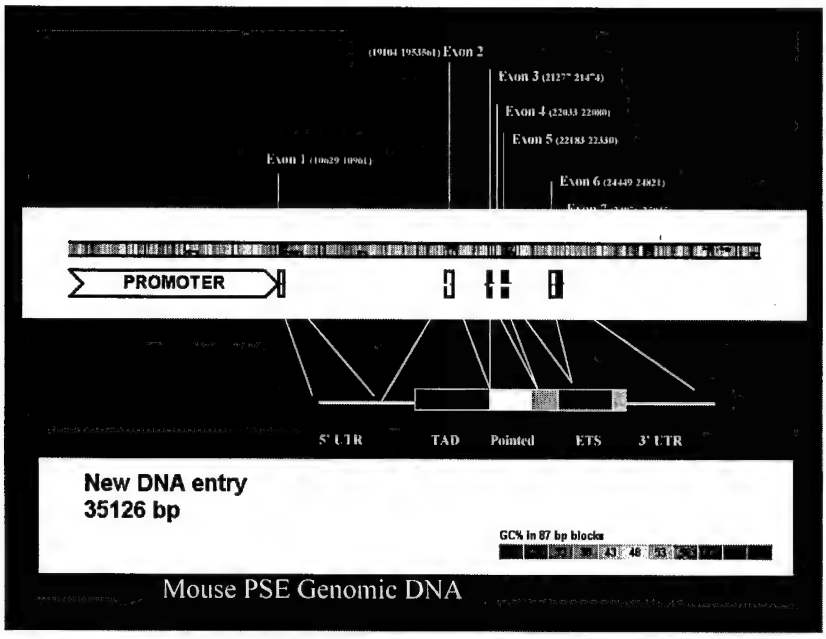

19. Progression to androgen-independent LNCAP human prostate tumors: cellular and molecular alterations

Jin-Rong Zhou, Lunyin Yu, Luiz F. Zerbini, Towia A. Libermann and George L. Blackburn. *Int. J.Cancer:110, 800-806,2004*

Lethal phenotypes of human prostate cancer are characterized by progression to androgen-independence and metastasis. For want of a clinically relevant animal model, mechanisms behind this progression remain unclear. Our study used an *in vivo* model of androgen-sensitive LNCaP human prostate cancer cell xenografts in male SCID mice to study the cellular and molecular biology of tumor progression. Primary tumors were established orthotopically, and the mice were then surgically castrated to withdraw androgens. Five generations of androgen-independent tumors were developed using castrated host mice. Tumor samples were used to determine expressions of cellular and molecular markers. Androgen-independent tumors had increased proliferation and decreased apoptosis compared to androgen sensitive tumors, outcomes associated with elevated expression of p53, p21/waf1, bcl-2, bax and the bcl-2/bax ratio. Blood vessel growth in androgen-independent tumor was associated with increased expression of vascular endothelial growth factor. Overexpression of androgen receptor mRNA and reduced expression of androgen receptor protein in androgen-independent tumors suggest that the androgen receptor signaling pathway may play an important role in the progression of human prostate cancer to androgen-independence. The *in vivo* orthotopic LNCaP tumor model described in our study mimics the clinical course of human prostate cancer progression. As such, it can be used as a model for defining the molecular mechanisms of prostate cancer progression to androgen-independence and for evaluating the effect of preventive or therapeutic regimens for androgen independent human prostate cancer.

20. Constitutive activation of NF-κB P50/P65 and AP-1 FRA-1 and JUND is essential for deregulated IL-6 expression in prostate cancer

Luiz F Zerbini, Yihong Wang, Je-Yoel Cho and Towia A Libermann. Cancer Research **63**:2206-15,2003

To date no effective treatment for patients with advanced androgen-independent prostate cancer is available, whereas androgen ablation therapy, surgery and radiation therapy are effective in treating local, androgen-dependent tumors. The mechanisms underlying the differences between androgen-dependent and –independent prostate cancer remain elusive. IL-6 is a pleiotropic cytokine whose expression under normal physiological conditions is tightly controlled. However, aberrant constitutive IL-6 gene expression has been implicated in prostate cancer progression and resistance

to chemotherapy, and has been directly linked to prostate cancer morbidity and mortality. Particularly striking is the large increase in the expression of IL-6 in hormone-refractory prostate cancer. IL-6, in addition to its role as an immunomodulatory cytokine, functions as a growth and differentiation factor for prostate cancer cells. To determine the molecular mechanisms that lead to deregulated IL-6 expression in advanced prostate cancer, we examined the regulatory elements involved in IL-6 gene expression in androgen-independent prostate cancer cells. We demonstrate that, in contrast to the androgen-sensitive LNCaP cells, androgen-insensitive PC-3 and DU145 cells express high levels of IL-6 protein and mRNA due to enhanced promoter activity. Deregulated activation of the IL-6 promoter is for the most part mediated by a combined constitutive activation of the NF-κB p50 and p65 and the AP-1 JunD and Fra-1 family members as demonstrated by electrophoretic mobility shift assays, site directed mutagenesis and transfection experiments. Mutation of the NF-κB and AP-1 sites drastically reduces IL-6 promoter activity in both androgen-independent prostate cancer cell lines. Additionally, inhibition of these transcription factors using adenovirus vectors encoding either the IκBα repressor gene or a dominant negative JunD mutant, leads to a strong downregulation of IL-6 gene expression at the mRNA and protein level as measured by real-time PCR and ELISA, respectively. Furthermore, the blockade of IL-6 gene expression results in drastic inhibition of the constitutively activated STAT3 signaling pathway in DU145 cells. Our data for the first time demonstrate that a combined aberrant activation of NF-κB p50 and p65 and AP-1 JunD and Fra-1 in androgen-independent prostate cancer cells results in deregulated IL-6 expression suggesting a novel potential entry point for therapeutic intervention in prostate cancer.

c. Key Research Accomplishments

- Chromosomal mapping and genomic organization of the human PDEF gene and identification of a functional promoter
- PDEF expression is strongly enhanced in human prostate cancer
- PDEF expression is induced by androgen
- Dominant-negative PDEF mutant specifically inhibits PDEF mediated transactivation of the PSA promoter
- Dominant-negative PDEF mutant specifically inhibits endogenous PSA gene expression in PSA positive LNCaP cells
- PDEF overexpression induces endogenous PSA gene expression in LNCaP cells
- TGF-β1 inhibits PDEF expression in prostate and breast cancer cell lines
- PDEF influences cell proliferation of LNCaP cells
- Characterization of PDEF target genes by oligonucleotide microarrays
- Generation of PDEF knockout vector and transfection into ES cells
- Identification and validation of target genes for PDEF by transcriptional profiling, real time PCR and siRNA interference
- PDEF phosphorylation by JNK and ERK MAP kinases
- Inhibition of PDEF expression induces apoptosis and cell cycle arrest of prostate cancer cells
- PDEF enhances prostate cancer tumor growth in SCID mice
- Inhibition of PDEF expression inhibits prostate cancer tumor growth in SCID mice
- Treatment of CaP cells with the NSAID Sulindac sulfide induces apoptosis and complete inhibition of PDEF expression
- PDEF overexpression enhances proliferation and growth of CaP cells in soft agar
- PDEF inhibits CaP cell migration and invasion, but enhances adhesion
- Inhibition of PDEF leads to morphological changes reminiscent of EMT

d. Reportable Outcomes

Adenoviral vectors for wild type and dominant-negative PDEF
SiRNA oligonucleotides for PDEF
Lentivirus encoding siRNA for PDEF

LNCaP and PC-3 cell clones stably transfected with wild type or dominant-negative PDEF or lentivirus with siRNA for PDEF
Expression vectors for wild type and dominant-negative PDEF
Polyclonal rabbit anti-PDEF antibody
Monoclonal mouse anti-PDEF antibody
PSA promoter luciferase constructs
Oligonucleotides for PDEF EMSA

e. Conclusions

Our grant was focused on evaluation of the role of the Ets transcription factor PDEF in prostate cancer development and progression and the potential to use PDEF for diagnostic or prognostic in prostate cancer. We have achieved the majority of the goals as outlined in our original proposal and our results have confirmed the relevance of PDEF for prostate cancer. Our results over the last three years have provided significant further evidence that PDEF is an important player in prostate as well as breast cancer. Immunohistochemistry confirmed our in situ hybridization experimnets, indicating enhanced expression of PDEF in prostate cancer tissue. Using overexpression of wild type as well as siRNA PDEF we confirmed in vitro as well as in animal studies that increased PDEF expression enhances tumor growth and that reduced PDEF expression inhibits tumor formation suggesting also that targeting PDEF may represent a therapeutic modality for prostate cancer. Using overexpression and RNA interefrence experiments we were able to identify PDEF target genes in microarray experiments of prostate cancer cells. These experiments demonstrated that PDEF regulates a variety of genes involved in migration and invasion, in particular genes involved in epithelial-mesenchymal transition (EMT) which plays an important role in development of metastasis. This was confirmed in a series of cell based assays of migration, invasion, proliferation and apoptosis. We demonstrated that PDEF expression is enhanced by androgen, but repressed by TGF-β and that PDEF overexpression enhances CaP proliferation and tumor growth in SCID mice. In contrast to PDEF overexpression, downregulation or inhibition of PDEF leads to EMT and regulation of a set of genes involved in adhesion, invasion, migration and cell cycle progression. PDEF may play two different roles in prostate cancer. Overexpression at early stages of prostate cancer may contribute to tumor formation and reduced expression at a later stage may trigger invasion and metastasis. Thus, PDEF may be a new prostate-specific target for both diagnostics and therapy in the ongoing battle to find a cure for CaP. Ultimately, we envision that PDEF will become a critical tool for the clinician as a diagnostic and prognostic marker and as a potential target for therapy in prostate cancer.

f. References

1: Zerbini LF, Wang Y, Cho JY, Libermann TA. Constitutive activation of nuclear factor kappaB p50/p65 and Fra-1 and JunD is essential for deregulated interleukin 6 expression in prostate cancer. Cancer Res. 2003 May 1;63(9):2206-15.

2: Zhou JR, Yu L, Zerbini LF, Libermann TA, Blackburn GL. Progression to androgen-independent LNCaP human prostate tumors: Cellular and molecular alterations. Int. J. Cancer 2004; 110 (6): 800-6.

AD_____
(Leave blank)

Award Number:

DAMD17-01-1-0023

APPENDICES:

1) List of personnel

2) Appended Publications (2)

Zhou, J-R., Yu, L., Zerbini, L., Libermann, T., Blackburn, G. Progression to Androgen-independent LNCAP Human Prostate Tumors: Cellular and Molecular Alterations. Int. J. Cancer: 110, 800-806 (2004)

Zerbini, L., Wang, Y., Cho, J-Y., Libermann, T. Constitutive Activation of Nuclear Factor kB p50/p65 and Fra-1 and JunD Is Essential for Deregulated Interleukin 6 Expression in Prostate Cancer. Cancer Research 63, 2206-2215, May 1, 2003

APPENDIX 1

AD_____
(Leave blank)

Award Number:

DAMD17-01-1-0023

LIST OF PERSONNEL:

TOWIA LIBERMANN, PH.D.	PRINCIPAL INVESTIGATOR
FRANCK GRALL, PH.D.	POSTDOCTORAL FELLOW
CHARLES BAILEY, B.S.	RESEARCH ASSISTANT

APPENDIX 2

Int. J. Cancer: **110**, 800–806 (2004)
© 2004 Wiley-Liss, Inc.

Publication of the International Union Against Cancer

PROGRESSION TO ANDROGEN-INDEPENDENT LNCAP HUMAN PROSTATE TUMORS: CELLULAR AND MOLECULAR ALTERATIONS

Jin-Rong ZHOU[1]*, Lunyin YU[1], Luiz F. ZERBINI[2], Towia A. LIBERMANN[2] and George L. BLACKBURN[1]

[1]*Nutrition/Metabolism Laboratory, Department of Surgery, Beth Israel Deaconess Medical Center, Harvard Medical School, Boston, MA, USA*

[2]*New England Baptist Bone & Joint Institute, The Genomics Center, Beth Israel Deaconess Medical Center, Harvard Medical School, Boston, MA, USA*

Lethal phenotypes of human prostate cancer are characterized by progression to androgen-independence and metastasis. For want of a clinically relevant animal model, mechanisms behind this progression remain unclear. Our study used an *in vivo* model of androgen-sensitive LNCaP human prostate cancer cell xenografts in male SCID mice to study the cellular and molecular biology of tumor progression. Primary tumors were established orthotopically, and the mice were then surgically castrated to withdraw androgens. Five generations of androgen-independent tumors were developed using castrated host mice. Tumor samples were used to determine expressions of cellular and molecular markers. Androgen-independent tumors had increased proliferation and decreased apoptosis compared to androgen-sensitive tumors, outcomes associated with elevated expression of p53, p21/waf1, bcl-2, bax and the bcl-2/bax ratio. Blood vessel growth in androgen-independent tumor was associated with increased expression of vascular endothelial growth factor. Overexpression of androgen receptor mRNA and reduced expression of androgen receptor protein in androgen-independent tumors suggest that the androgen receptor signaling pathway may play an important role in the progression of human prostate cancer to androgen-independence. The *in vivo* orthotopic LNCaP tumor model described in our study mimics the clinical course of human prostate cancer progression. As such, it can be used as a model for defining the molecular mechanisms of prostate cancer progression to androgen-independence and for evaluating the effect of preventive or therapeutic regimens for androgen-independent human prostate cancer.
© *2004 Wiley-Liss, Inc.*

Key words: *prostate cancer; androgen-sensitive; androgen-independent; orthotopic model*

Prostate carcinoma is the second leading cause of cancer death in American men, with 1 in every 5 patients developing invasive cancer. It accounts for an estimated 29% of all new cancer cases diagnosed in U.S. men.[1] Most prostate cancer is initially androgen-dependent (AD). In 80% of men who receive androgen blockade therapy, cancer cells die and patients show improvement. In time, however, nearly all tumors grow back to androgen-independence (AI). Clinically, the lethal phenotypes of human prostate cancer are characterized by progression to androgen-independence.[2]

The search for effective therapies for prostate cancer and in particular for ways to intervene in the progression of AI tumors has been hampered by a lack of clinically relevant animal models. The ability to validate new concepts requires representative model systems of human origin that mimic the clinical process of the disease in patients. In some animal models, prostate tumors have been developed and progressed subcutaneously, therefore tumor-host interactions in these models are different from that in humans. Coinoculation of tumor cells with specific fibroblasts (*e.g.*, prostate and bone fibroblasts) has improved tumor cell-host cell interaction.[3,4] An *in vivo* orthotopic prostate tumor model, which mirrors tumor cell-host interactions in humans, is considered even more relevant.[5,6]

Our understanding of the mechanisms of progression of AD prostate cancer to AI prostate cancer has been largely obtained through the study of experimental animal models. The cellular and molecular responses of AD tumors to androgen ablation have been described in studies using *in vivo* animal models that mimic the progression of prostate cancer after surgical castration.[4,7–9] Previous animal studies have produced inconsistent and contradictory findings on the effects of androgen withdrawal on tumor AR expression,[4,8,10–14] apoptosis[7–9] and proliferation.[7–9] These results suggest that tumor cell biology as well as nonandrogenic variables (*e.g.*, extracellular matrix pathways or altered growth factors) may play roles in the regulation of prostate cancer progression and the modulation of cellular and molecular events.[3,4,15]

In our study, we developed an *in vivo* animal model of human prostate cancer progression from androgen-sensitive (AS) to AI by surgical castration of SCID mice bearing orthotopic LNCaP human prostate tumor. This *in vivo* androgen-sensitive prostate tumor model resembles tumor-stromal interactive microenvironments in humans. To investigate the effects of androgen withdrawal on cellular and molecular markers, we grew 5 generations of AI tumors in castrated host animals. We established that this *in vivo* orthotopic model of AI tumor progression has clinical relevance in the evaluation of preventive or therapeutic regimens for AI human prostate cancer.

MATERIAL AND METHODS

Orthotopic implantation of LNCaP tumor cells

Eight-week-old male SCID beige mice were purchased from Taconic (Germantown, NY) and housed in a pathogen-free environment. Immediately before implantation, exponentially growing LNCaP cells were trypsinized and resuspended in DMEM with 10% FBS, cell viability was determined by Trypan blue exclusion, and a single-cell suspension with >90% viability was used for implantation. A transverse incision was made in the lower abdomen, and the bladder and seminal vesicles were delivered through the incision to expose the dorsal prostate. LNCaP cells (2×10^6 cells in 50 μL medium) were carefully injected under the prostatic capsule via a 30-gauge needle. Proper inoculation of cell suspension was indicated by blebbing under the prostatic capsule. The incision was closed using a running suture of 5-0 silk. All proce-

Abbreviations: AD, androgen-dependent; AI, androgen-independent; AR, androgen receptor; AS, androgen-sensitive; PSA, prostate-specific antigen; TUNEL, terminal deoxynucleotidyl transferase-mediated dUTP-biotin nick end labeling; RT-PCR, reverse transcription-polymerase chain reaction; VEGF, vascular endothelial growth factor.

*Correspondence to: Nutrition/Metabolism Laboratory, Department of Surgery, Beth Israel Deaconess Medical Center, Harvard Medical School, 330 Brookline Avenue, Burlington-554B, Boston, MA 02215. Fax: +617-632-0275. E-mail: jrzhou@bidmc.harvard.edu

Received 24 July 2003; Revised 31 December 2003; Accepted 13 January 2004

DOI 10.1002/ijc.20206

Published online 24 March 2004 in Wiley InterScience (www.interscience.wiley.com).

dures with animals were reviewed and approved by the Institutional Animal Care and Use Committee at Beth Israel Deaconess Medical Center according to the NIH guidelines.

Establishment and passage of AI prostate cancer

When the AS tumor was developed, androgen withdrawal was accomplished by surgical castration. The AS tumor regressed initially in response to androgen ablation and then regrew to develop the AI tumor (the first generation, abbreviated as AI-1), as monitored by increase of serum prostate-specific antigen (PSA) and tumor volume. The AI-1 tumor was then orthotopically implanted into castrated SCID host mice to develop the second generation of the AI tumor (AI-2). This process was repeated 3 more times so that the third (AI-3), the forth (AI-4) and the fifth (AI-5) generation of AI tumor sublines were developed. Biologic samples from at least 4 mice in each generation were collected for analysis.

Tumor histology

For histologic examination, tumor tissues were fixed in 10% buffered neutralized formalin, embedded in paraffin, cut into 5 μm sectiona and stained with hematoxylin-eosin.

In situ *detection of apoptotic index*

Apoptotic cells were determined by a terminal deoxynucleotidyl transferase-mediated dUTP-biotin nick end labeling (TUNEL) assay using the ApopTag plus peroxidase *in situ* apoptosis detection kit (Intergen, Purchase, NY) according to our previous procedures.[6,16] Six representative areas of each section without necrosis were selected, and both apoptotic cells and total nuclei cells were counted under a light microscope at 400× magnification. The apoptotic index was expressed as the percentage of positive apoptotic tumor cells to total tumor cells.

Tumor blood vessel

Six nonnecrotic and nonblooded fields in each H&E-stained tumor specimen were selected, and visible blood vessels within the same area were counted under microscope at 200× magnification.

Immunohistochemical determinations of AR, p53, p21/wafl and Ki-67

Automated immunohistochemistry followed by image analysis was applied to quantify the expression of AR, p53, p21/wafl and Ki-67, according to our previously described procedures.[6] In brief, after deparaffinization, rehydration and washing, the section was soaked in 10 mM citrate buffer (pH 6.0) and heated for 20 min in a microwave oven. After being cooled to room temperature, the section was treated with 1% hydrogen peroxide for 5 min, then stained by using an automated staining machine (ES; Ventana Medical Systems, Tucson, AZ). The section was incubated with the primary antibody for 32 min and incubated with a biotinylated universal anti-mouse/rabbit IgG (VECTASTAIN, 1:100 dilution). The section was then stained with 3-3′ diaminobenzidine and counterstained with hematoxylin and a bluing agent by using 3-3′ diaminobenzidine Detection Kit (Ventana Medical Systems). Digital images of 5 fields in each tissue section were acquired at 400× magnification with a digital camera (CoolSNAP; RS Photometrics, Tucson, AZ) mounted on a light microscope (Leica DMLS; Leica Microsystems Wetzlar, Ernst-Leitz-Strasse, Germany). True-color image analysis was performed by using IPLab 3.5 image analysis software (Scanalytics, Fairfax, VA) to quantify the percentages of positive tumor cells to total tumor cells. Both positive- and negative-control slides were used to confirm the sensitivity and specificity of staining. The antibodies and dilutions were as follows: a mouse anti-human AR monoclonal antibody (1:50, Clone AR441, DAKO, Carpinteria, CA), a mouse anti-human p53 monoclonal antibody (1:100, DO-1, reactive with both wild and mutant p53; Santa Cruz Biotechnology, Santa Cruz, CA), a mouse anti-human p53 monoclonal antibody (1:25, Pab 240, reactive with mutant p53 only, Santa Cruz Biotechnology), a mouse anti-human p21/wafl monoclonal antibody (1:100, AB-1; Calbiochem, San Diego, CA), a mouse anti-human Ki-67 monoclonal antibody (1:20, Ki-S5; DAKO).

Immunohistochemical determination of proliferation index

Ki-67 was determined by immunohistochemical staining to quantify the proliferation index, as described above. Both Ki67-positive proliferating cells and total tumor cells were counted in 3 nonnecrotic areas of each section using light microscopy at 400× magnification. The proliferation index was calculated as the percentage of Ki-67-positive tumor cells to total tumor cells.

Western blot analysis

Western blot analysis was performed to determine the expression of bcl-2, bax and vascular endothelial growth factor (VEGF). The housekeeping protein GAPDH was used as the control. Total tumor cell lysate was prepared by extracting total cellular proteins with lysis buffer [PBS, pH 7.4, 1% NP-40, 0.5% sodium deoxycholate, 0.1% SDS] and with freshly added proteinase inhibitors [10 mM N-ethylmaleimide, 10 μg/mL aprotinin, 2 μg/mL pepstatin A, 10 μg/mL leupeptin, 2 mM phenylmethylsulfonyl fluoride, 1.0 mM $NaVO_4$, 10 mM NaF], followed by centrifugation. Western blotting was performed based on standard procedures. In brief, proteins (50 μg) were separated by SDS-polyacrylamide gel and transferred onto polyvinylidene difluoride membrane. After blocking nonspecific sites by 5% milk overnight (nonfat dry milk in PBS), the membrane was incubated with primary antibodies for 60 min, washed and incubated with horseradish peroxidase-conjugated secondary antibody (1:2,000; Amersham Life Science, Arlington Heights, IL). Primary antibodies used for Western blot analysis were anti-Bcl-2 monoclonal (1:50, clone 124; DAKO), anti-bax monoclonal (1:50, AB-1; Oncogene), anti-VEGF monoclonal (2.5 μg/ml AB-2; Oncogene) and anti-GAPDH monoclonal (0.1 μg/ml, Clone 6C5; Research Diagnostics, Flanders, NJ). Western blots were developed using the chemiluminescent reagent (ECL; Amersham Life Science) according to the manufacturer's instructions. The levels of protein expression were quantified by densitometry using Bio-Rad GS-700 Imaging Densitometer (Bio-Rad Laboratory, Hercules, CA) and NIH image analysis program (NIH Image 1.62).

Reverse transcription-PCR (RT-PCR)

AR mRNA was determined by RT-PCR. Total RNA was extracted from tumor tissues using the RNeasy Mini Kit (Qiagen, Valencia, CA) according to the manufacturer's protocol. cDNA was prepared using Ready-To-Go, You-Prime First-Strand Beads (Amersham Pharmacia, Piscataway, NJ). The primer pairs for AR (5′-AGA TGG GCT TGA CTT TCC CAG AAA G-3′ and 5′-ATG GCT GTC ATT CAG TAC TCC TGG A-3′) and for GAPDH (5′-CAAAGT TGT CAT GGA TGA CC-3′ and 5′-CCA TGG AGA AGG CTG GGG-3′) were purchased for PCR from Invitrogen Life Technologies (Frederick, MD). PCR was performed according to standard procedures by using Eppendorf Mastercycler (Eppendorf Scientific, Westbury, New York). Thermal cycling was performed by initial denaturation at 94°C for 2 min, followed by 40 cycles according to the following cycle profile: denaturation at 94°C for 45 sec, annealing at 50°C for 45 sec and elongation at 72°C for 1 min. After PCR, electrophoresis was run to ensure that a right-size product was amplified in the reaction by using Tris/EDTA (TAE)-buffered agarose gels (1.5%). NIH Image 1.62 software was used to quantify the expression of AR mRNA.

Statistical analysis

All data were expressed as group means ± SEM. Data were analyzed by analysis of variance followed by Fisher's protected least-significant difference[17] using Statview 5.0 program (SAS Institute, Cary, NC). A p-value < 0.05 was considered as statistically significant.

RESULTS

Effects of AI tumor progression on tumor growth, metastasis and histology

We have developed an *in vivo* model of AI prostate cancer from AS prostate cancer by using intraprostatic inoculation of LNCaP human prostate cancer cells in mice. Castration initially inhibited the orthotopic growth of LNCaP tumor and lowered serum PSA levels. Tumors then started to grow again in the absence of testicular androgen to develop the AI tumor. The time required for tumor to regrow to AI was dependent upon the size of AS tumor before castration. The AI tumor was then harvested and orthotopically implanted to the castrated host mouse to develop a total of 5 generations of the AI tumor. During development of the AI tumors, the rates of tumorigenicity were 100%. AI tumors grew faster with each generation. The average time required for AI-1 tumor development was about twice as that for AI-4 and AI-5 tumor development.

Serum level of PSA was measured by ELISA assay. AI tumors secreted PSA to blood, and PSA levels were associated with tumor size. Since tumors were not collected at the same size or the same time, the comparisons of serum PSA levels between different generations of tumors were less meaningful and thus were not performed. The metastasis rate was not evaluated because of the small number of samples ($n = 4$ for each group).

Effects of AI tumor progression on AR expression

The effects of androgen withdrawal on the expression of AR transcript and protein were determined by RT-PCR and immunohistochemistry, respectively. Compared to the AS tumors (Fig. 1*a*), the AI tumors had reduced expression of AR protein (Fig. 1*b*). Almost all of the AS tumor cells (92.6%) were AR-positive. But the percentages of AR-positive cells in different generations of AI tumors were gradually reduced from 83.3% ($p < 0.05$), 76.2% ($p < 0.01$), 59.1% ($p < 0.01$), 63.6 % ($p < 0.01$) to 59.2% ($p < 0.01$) (Fig. 1*c*).

In contrast to AR protein expression, RT-PCR analysis indicated that the AI tumors had increased expression of AR mRNA compared to the AS tumor (Fig. 1*d*). There were no differences of AR mRNA expressions between AI tumors. Image analysis showed that the AR mRNA expressions in the AI tumors were twice as that in the AS tumors ($p < 0.05$).

Effects of AI tumor progression on cell proliferation

Ki-67 staining was used to determine the prostate cancer cell proliferation index. The AI tumor progression significantly increased tumor cell proliferation. The proliferation indices in the AI-1, AI-2, AI-3, AI-4 and AI-5 tumor cells were increased by 122% ($p < 0.05$), 133.5% ($p < 0.05$), 139.0% ($p < 0.05$), 122.6% ($p < 0.05$) and 123.8% ($p < 0.05$), respectively, compared to that of the AS tumor (Table I). There were no further significant changes of cell proliferation among AI tumors (Table I).

Effects of AI tumor progression on apoptosis and the expression of apoptosis modulators

The TUNEL assay was used to determine the *in situ* apoptosis of prostate tumor cells. The apoptotic index in the AI-1 tumor was significantly inhibited by 72% ($p < 0.01$), and there were no further significant changes of apoptosis in subsequent AI tumors (Table I).

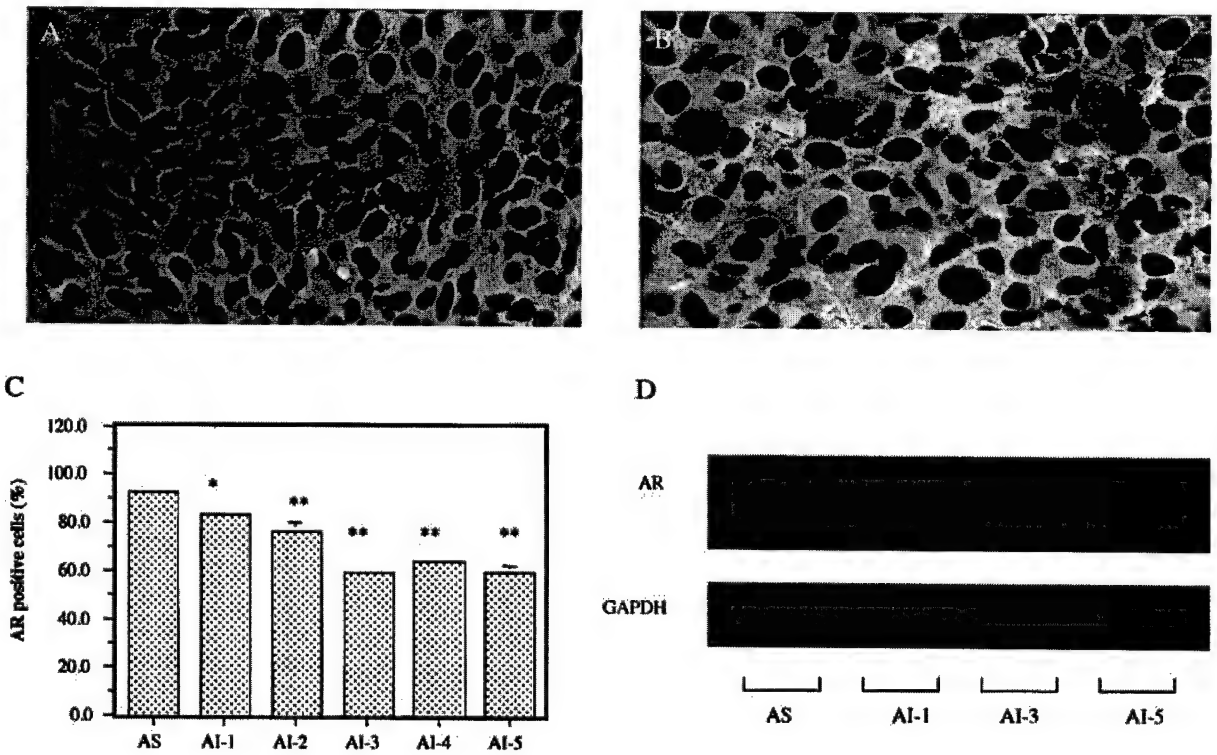

FIGURE 1 – Effects of androgen-independent (AI) tumor progression on androgen receptor (AR) expression. AR protein was immunohistochemically detected in the androgen-sensitive (AS) tumor *(a)* and in the androgen-independent (AI) tumor *(b)* (original magnification, ×400). AR-positive cells were stained brown. The percentages of AR-positive tumor cells were 92.6% in the AS tumor and were decreased from 83.3%to 59.2% in the AI-1 to AI-5 tumors *(c)*. Values with asterisks are significantly different from the AS control (*$p < 0.05$; **$p < 0.01$). RT-PCR analysis indicated that the AI tumors had increased expression of AR mRNA compared to the AS tumor *(d)*. Values are expressed as means ± SEM. For each generation, $n = 4$.

TABLE I – EFFECTS OF AI TUMOR PROGRESSION ON TUMOR CELL PROLIFERATION, APOPTOSIS AND EXPRESSION OF P53 AND P21/WAF1

Treatment	Proliferation index (% total cells)	Apoptotic index (% total cells)	p53		p21/waf1	
			Positive cells (% total cells)	Intensity (% AS tumor)	Positive cells (% total cells)	Intensity (% AS tumor)
AS	16.4 ± 8.1	9.99 ± 0.75	6.8 ± 2.6	100.0	3.89 ± 1.19	100.0
AI-1	36.4 ± 2.5[1]	2.79 ± 0.78[2]	9.5 ± 0.6	130.5 ± 8.6[2]	15.97 ± 6.12[1]	154.3 ± 4.3[2]
AI-2	38.3 ± 4.0[1]	3.96 ± 0.17[2]	30.1 ± 5.8[2]	139.7 ± 1.4[2]	13.56 ± 2.60	165.0 ± 0.2[2]
AI-3	39.2 ± 5.2[1]	4.19 ± 0.25[2]	27.3 ± 1.6[2]	145.6 ± 2.1[2]	21.39 ± 0.97[2]	167.2 ± 0.4[2]
AI-4	36.5 ± 8.4[1]	2.84 ± 0.19[2]	28.1 ± 1.4[2]	153.0 ± 4.5[2]	18.46 ± 2.32[1]	168.9 ± 2.6[2]
AI-5	36.7 ± 1.4[1]	2.66 ± 0.75[2]	29.9 ± 0.5[2]	149.6 ± 7.0[2]	12.78 ± 2.54	165.8 ± 0.8[2]

Values are means ± SD.–AI, androgen-independent; AS, androgen-sensitive–[1]Value is significant from that of the AS tumor, $p < 0.05$.–[2]Value is significant from that of the AS tumor, $p < 0.01$.

The expressions of the apoptosis promoters p53, p21/wafl and Bax and the apoptosis inhibitor bcl-2 in tumors were detected by immunohistochemistry or Western blot to further elucidate the molecular mechanisms by which the development of AI prostate cancer modulates tumor cell apoptosis. The p53-positive cells in the AI-1, AI-2, AI-3, AI-4 and AI-5 tumors increased 39.7% ($p > 0.05$), 342.6% ($p < 0.01$), 301.5% ($p < 0.01$), 313.2% ($p < 0.01$) and 339.7% ($p < 0.01$), respectively, compared to the AS tumors (Table I). In addition to increased numbers of p53-positive cells, the AI tumors also had significantly increased intensity of p53 expression in p53-positive cells by 30.5% to 53% ($p < 0.01$, Table I). Similar to p53, the p21/waf1-positive cells in the AI-1, AI-2, AI-3, AI-4 and AI-5 tumors increased by 310.5% ($p < 0.05$), 248.6% ($p > 0.05$), 449.9% ($p < 0.01$), 374.6% ($p < 0.05$) and 228.5% ($p > 0.05$), respectively (Table I). The intensities of p21/waf1 protein in p21/wafl-positive cells also significantly increased by 54.3% to 68.9% in the AI tumors ($p < 0.01$).

Both bcl-2 and bax proteins were significantly higher in the AI tumors than that in the AS tumors (Fig. 2*a*). The increase of bcl-2 expression was higher than that of Bax, resulting in significant 3–7-fold increases of bcl-2/Bax ratios in the AI tumors (Fig. 2*b*).

Effects of AI tumor progression on blood vessel formation and the expression of angiogenic factor VEGF

The number of blood vessels in tumors were counted in H&E-stained slides. The AI tumor showed more blood vessels than the AS tumor (Fig. 3*a*). Compared to that of the AS tumor, the blood vessel numbers in the AI-1, AI-2, AI-3, AI-4 and AI-5 tumors were significantly increased by 129% ($p < 0.01$), 200% ($p < 0.01$), 213% ($p < 0.01$), 367% ($p < 0.01$) and 288% ($p < 0.01$), respectively. In parallel, Western blot analysis indicated that the AI tumor progression significantly increased VEGF expression by 0.5–3-fold in the AI tumors, compared to that in the AS tumors (Fig. 3*b,c*).

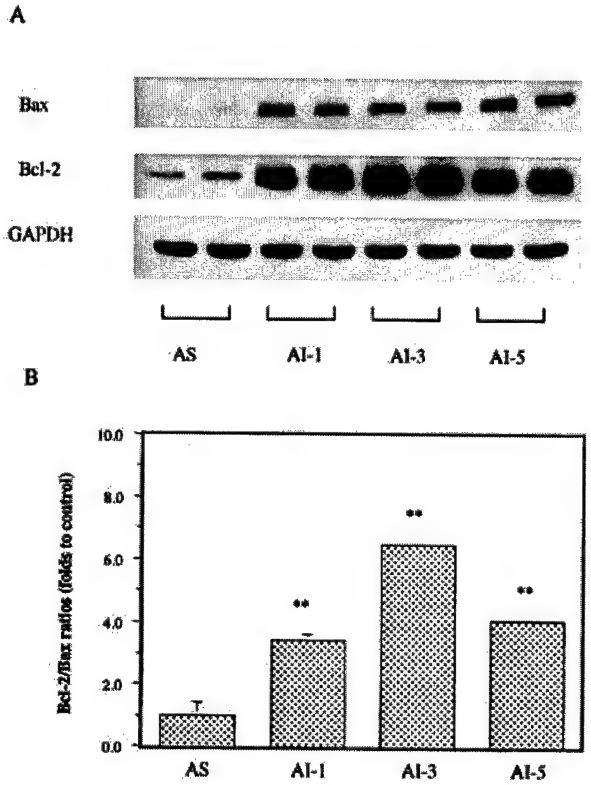

FIGURE 2 – Effects of androgen-independent (AI) tumor progression on the expression of bax and bcl-2 proteins. Both bcl-2 and bax proteins were significantly higher in the AI tumors than that in the androgen-sensitive (AS) tumors *(a)*. The increase of bcl-2 expression was higher than that of bax, resulting in significant 3-fold to 7-fold increases of bcl-2/Bax ratios in the AI tumors *(b)*. Values with asterisks are significantly different from the AS control (**$p < 0.01$). Values are expressed as means ± SEM.

DISCUSSION

In our study, we used an orthotopic animal model of AS human LNCaP prostate cancer progression to mimic the tumor cell-host cell interactive microenvironments and evaluate cellular and molecular changes during AI tumor progression. We also grew orthotopic AI tumors in up to 5 generations of castrated host animals. Progression to androgen independence was associated with increased proliferation and reduced apoptosis of prostate cancer cells. We also determined mRNA and protein expression of AR using RT-PCR and immunohistochemistry, respectively. Results (Fig. 1*d*) showed a 2-fold increase in expression of AR mRNA in all 5 generations of AI tumors and a gradual decline in expression of AR protein, by 10% from the AI-1 tumor to 36% by the AI-5 tumor. These findings indicate that androgen withdrawal may have the opposite effect on AR transcription and translational or post-translational modification processes, and AI progression is associated with a reduction of AR function.

To be clinically relevant, animal models must meet certain strict criteria, *i.e.*, tumor cell maintenance of key biologic traits of the human prostate, such as secretion of PSA; sensitivity to or dependence on androgen for growth; AI tumor development from an AD carcinoma after androgen withdrawal; and growth of primary tumor cells in the relevant environment. Thalman *et al.* found that unlike other human prostate cancer models, the LNCaP progression model shares remarkable similarities with human prostate cancer.[2] Orthotopic LNCaP tumor model mirrors tumor cell-host interactions in humans and is considered more clinically relevant.[5,6] This orthotopic SCID-LNCaP tumor model was used in our study to determine the alterations of tumor markers associated with progression of AI prostate tumors after androgen ablation treatment, therefore the results were expected to be significant clinically.

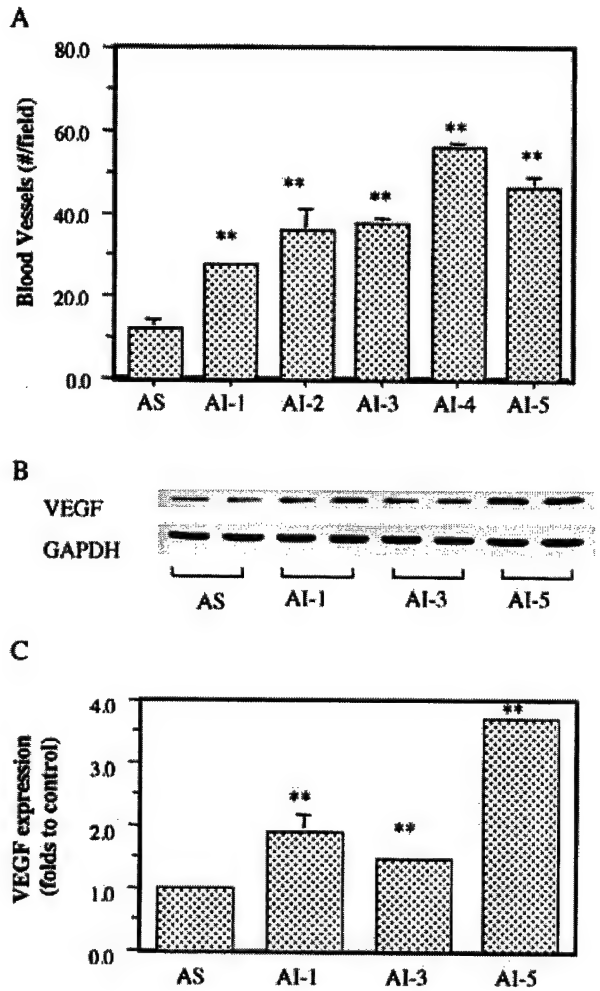

Figure 3 – Effects of androgen-independent (AI) tumor progression on blood vessel formation and VEGF expression. *(a)* Blood vessel numbers in the androgen-sensitive (AS) and AI tumors. *(b)* Western blot analysis of VEGF expression in the AS and AI tumors. *(c)* Quantification of VEGF expression. Values with asterisks are significantly different from the AS control (**$p < 0.01$).

The molecular mechanisms that underlie the transition of prostate tumors from AS to AI status remain unknown. Evidence suggests that the AR signaling pathway could play a central role.[18] AR expression occurred in both kinds of tumors,[19,20] but the levels of expression were found to vary. Some studies reported increased expression of AR in hormone-refractory AI tumors; [10–13,21,22] others, however, found decreased expression of AR in AI tumors.[14,19,23,24] In reviewing the literature, we found that the studies reporting increased expression of AR were those determining AR mRNA expressions, and that the studies reporting decreased expression of AR were those determining AR protein expression. Unfortunately, previous research measured either mRNA or AR protein. In our study, we determined both mRNA and protein expression of AR. Results showed that AR mRNA expression was increased 2-fold in all 5 generations of AI tumors, whereas AR protein expression was decreased gradually from the AI-1 tumor to the AI-5 tumor (Fig. 1*c,d*). Our results provide evidence to understand the nature of AR modulation by androgen ablation in prostate cancer progression. Our results, together with others, suggest that AI tumor progression due to androgen ablation is associated with increased AR transcript but with decreased AR protein. Additional studies on how androgen ablation alters AR transcription and translation may further elucidate the tumor progression process and facilitate the development of novel therapies.

Clinical progression of prostate cancer after hormonal therapy is usually associated with reduced apoptosis and increased proliferation of prostate cancer cells. Androgen ablation treatment induced initial apoptosis in AD prostate cancer.[25] Progression of AI tumors was associated with significant reductions in apoptosis and nonsignificant increases (23%) in proliferation compared to AD tumors[26,27] and that the low apoptotic index in primary prostate tumor was associated with poor response to hormonal therapy.[27] Conversely, findings from animal studies are inconsistent. Bladou *et al.*[9] found a decrease in the proliferation index after castration and progression of the AI tumor; a significant drop in tumor growth rate, followed by an increase; and an initial rise in the apoptotic index, followed by a decline; the AI tumor relapse after castration was associated with a reduced apoptosis with no increase in proliferation.[9] Landstrom *et al.*[7] reported an association between regrowth of AI prostate tumors and a reduction in apoptosis; AI tumor regrowth was not, however, associated with increased cell proliferation. Agus *et al.*[8] found that androgen withdrawal produced an initial decrease in prostate cancer cell proliferation, followed by increases consistent with AI tumor regrowth; apoptosis remained unchanged during regression and regrowth. Therefore, more studies are needed by using clinically relevant animal models to characterize alterations of tumor markers associated with androgen ablation and progression to AI tumors.

Our study describes an association between regrowth of AI tumors and both decreased apoptosis and increased proliferation of tumor cells. Results (Table I) also showed maintenance of apoptosis and proliferation rates from the first to the fifth generations of AI tumors. These results, which are consistent with clinical findings,[26,27] suggest that our animal model for orthotopic AI tumor progression could provide a clinically relevant *in vivo* model of AI tumor progression for studies of apoptosis and proliferation mechanisms.

Molecular mechanisms behind the modulation of tumor apoptosis and proliferation by androgen withdrawal have been studied extensively. Apoptosis is a major physiologic means of cell removal, a process that involves many molecular modulators, such as bcl-2, bax, p53 and p21/WAF1. Proteins encoded by bcl-2 family genes are important regulators of apoptosis. Expression of bcl-2 tended to be more frequent in high-grade tumors and metastases than in lower-grade and nonmetastatic tumors.[28,29] Apoptosis resistance was associated with higher levels of bcl-2.[29,30] Overexpression of bcl-2 after androgen ablation was correlated with the progression of prostate cancer from androgen dependence to androgen independence.[31] These findings suggest that bcl-2 protein might be a factor that enables prostate cancer cells to survive in androgen-deprived environments. The tumor suppressor gene p53, known to be involved in the regulation of cell growth and apoptosis, was implicated in hormone refractory prostate cancer and poor prognosis. p53 protein accumulation and mutation were associated with increased cell proliferation rate, increased histologic grade and stage and transition from AD to AI growth.[32] Metastatic and hormone-refractory tumors showed increased p53 protein expression associated with p53 gene alterations.[33–35] Both bcl-2 and p53 protein accumulations were observed in hormone-refractory prostate cancer.[35] Clinically, patients who showed overexpression of bcl-2 or p53 had a significantly higher 5-year failure rate than those who don't.[36]

Our study described increased expression of p53 (Table I) and bcl-2 proteins (Fig. 2) in AI tumors, findings consistent with clinical observations. It has been suggested that the bcl-2/bax ratio might be a better indicator of tumor apoptosis than p53 or bcl-2 protein accumulations.[37] In our study, we observed increased expression of both bcl-2 and bax. The rise in bcl-2 expression,

however, was much higher than that in bax. In turn, bcl-2/bax ratios were 3–6-fold higher in the different generations of AI tumors (Fig. 2). These results, which mirror clinical findings, suggest that our animal model of orthotopic AI tumor progression can be used as a clinically relevant *in vivo* model for investigation of the molecular mechanisms by which androgen ablation leads to progression of AI tumors.

Human prostate tumors are dependent on angiogenesis for growth, and VEGF is a major regulator of this process. Androgens upregulated VEGF expression, and hormone-ablation-induced tumor-growth inhibition was associated with a decrease in VEGF expression and markedly reduced tumor neovascularization.[38–40] However, relapse of prostate tumors after androgen-ablation therapy was associated with increased angiogenesis and VEGF expression.[41] By using an orthotopic prostate tumor model, we found that the progression of AI prostate tumor was associated with increased tumor vascularization and expression of VEGF. It suggests that our animal model of can be used as a clinically relevant *in vivo* model for investigation of the molecular mechanisms by which relapse of androgen ablation treatment leads to increased angiogenesis and VEGF expression and for evaluation the efficacy of the anti-angiogenic therapy on progression of AI prostate tumor.

In our study, up to 5 generations of AI tumors were used to characterize the alteration of tumor markers associated with androgen ablation and progression of AI tumors. The comparison of biomarkers in different generations of tumors provided important information on understanding the long-term effects of androgen ablation treatment on tumor marker modulation. As our results show, both tumor cell proliferation and apoptosis indices, two primary parameters that are associated with development of androgen independence of prostate tumor, were significantly altered in AI-1 tumors compared to the AS tumors, and no further alterations were observed in other generations of AI tumors. AI-1 tumors also showed significantly more blood vessels than the AS tumors, although more blood vessels were present in the later generations of the AI tumors. This observation is consistent with the clinical observation that development of the AI tumor is associated with increased angiogenesis. Even though different molecular markers may have had slightly different time-dependent responses to androgen ablation, all markers showed similar trends of alteration among different AI tumors, suggesting that alterations of these molecular markers are consistent with that of the cellular markers. These results suggest that AI-1 tumor is sufficient to represent the androgen-independent prostate tumor.

In conclusion, hormone withdrawal-induced AI tumor progression was associated with increased proliferation and decreased apoptosis of prostate tumor cells, increased expressions of p53, bcl-2 and bcl-2/bax ratios, increased tumor vascularization and VEGF expression and the decreased AR protein/function. The *in vivo* orthotopic LNCaP tumor model described in our study mimics the clinical course of human prostate cancer. As such, it can be used as a model for defining the molecular mechanisms of prostate cancer progression and for evaluating the efficacy of treatment for AI/hormone-refractory prostate cancer.

ACKNOWLEDGEMENTS

This work was supported in part by Massachusetts Department of Public Health Prostate Cancer Research Program, RO3 CA 10104 (National Cancer Institute, NIH) and RO1 CA 78521 (National Cancer Institute, NIH) [to J-RZ] and by DAMD 170110023 (U.S. Army) and RO1 CA 85467 (National Cancer Institute, NIH) [to TAL].

REFERENCES

1. Landis SH, Murray T, Bolden S, Wingo PA. Cancer Statistics. CA Cancer J Clin 1999;49:8–31.
2. Thalmann GN, Sikes RA, Wu TT, Degeorges A, Chang SM, Ozen M, Pathak, S, Chung LW. LNCaP progression model of human prostate cancer: androgen-independence and osseous metastasis. Prostate 2000;44:91–103.
3. Gleave ME, Hsieh JT, Gao C, Chung LWK, von Eschenbach AC. Acceleration of human prostate cancer growth in vivo by prostate and bone fibroblasts. Cancer Res 1991;51:3753–61.
4. Wu HC, Hsieh JT, Gleave ME, Brown NM, Pathak S, Chung LW. Derivation of androgen-independent human LNCaP prostatic cancer cell sublines: role of bone stromal cells. Int J Cancer 1994;57:406–12.
5. Sato N, Gleave ME, Bruchovsky N, Rennie PS, Beraldi E, Sullivan LD. A metastatic and androgen-sensitive human prostate cancer model using intraprostatic inoculation of LNCaP cells in SCID mice. Cancer Res 1997;57:1584–9.
6. Zhou J-R, Yu L, Zhong Y, Nassr RL, Franke AA, Gaston SM, Blackburn GL. Inhibition of orthotopic growth and metastasis of androgen-sensitive human prostate tumors in mice by bioactive soybean components. Prostate 2002;53:143–53.
7. Landstrom M, Damber J-E, Bergh A. Prostatic tumor regrowth after initially successful castration therapy may be related to a decreased apoptotic cell death rate. Cancer Res 1994;54:4281–4.
8. Agus DB, Cordon-Cardo C, Fox W, Drobnjak M, Koff A, Golde DW, Scher HI. Prostate cancer cell cycle regulators: response to androgen withdrawal and development of androgen independence. J Natl Cancer Inst 1999;91:1869–76.
9. Bladou F, Vessella RL, Buhler KR, Ellis WJ, True LD, Lange PH. Cell proliferation and apoptosis during prostatic tumor xenograft involution and regrowth after castration. Int J Cancer 1996;67:785–90.
10. Koivisto P, Kononen J, Palmberg C, Tammela T, Hyytinen E, Isola J, Trapman J, Cleutjens K, Noordzij A, Visakorpi T, Kallioniemi, OP. Androgen receptor gene amplification: a possible molecular mechanism for androgen deprivation therapy failure in prostate cancer. Cancer Res 1997;57:314–9.
11. Linja MJ, Savinainen KJ, Saramaki OR, Tammela TL, Vessella RL, Visakorpi T. Amplification and overexpression of androgen receptor gene in hormone-refractory prostate cancer. Cancer Res 2001;61: 3550–5.
12. Bubendorf L, Kononen J, Koivisto P, Schraml P, Moch H, Gasser TC, Willi N, Mihatsch MJ, Sauter G, Kallioniemi OP. Survey of gene amplifications during prostate cancer progression by high-throughout fluorescence in situ hybridization on tissue microarrays. Cancer Res 1999;59:803–6.
13. Miyoshi Y, Uemura H, Fujinami K, Mikata K, Harada M, Kitamura H, Koizumi Y, Kubota Y. Fluorescence in situ hybridization evaluation of c-myc and androgen receptor gene amplification and chromosomal anomalies in prostate cancer in Japanese patients. Prostate 2000;43:225–32.
14. Kinoshita H, Shi Y, Sandefur C, Meisner LF, Chang C, Choon A, Reznikoff CR, Bova GS, Friedl A, Jarrard DF. Methylation of the androgen receptor minimal promoter silences transcription in human prostate cancer. Cancer Res 2000;60:3623–30.
15. Chung LW, Li W, Gleave ME, Hsieh JT, Wu HC, Sikes RA, Zhau HE, Bandyk MG, Logothetis CJ, Rubin JS. Human prostate cancer model: roles of growth factors and extracellular matrices. J Cell Biochem Suppl 1992;16H:99–105.
16. Zhou J-R, Gugger ET, Tanaka T, Guo Y, Blackburn GL, Clinton SK. Soybean phytochemicals inhibit the growth of transplantable human prostate carcinoma and tumor angiogenesis in mice. J Nutr 1999;129: 1628–35.
17. Steel RGD, Torrie JH. Principles and procedures of statistics: a biometrical approach, 2nd ed. New York: McGraw-Hill, 1980.
18. Grossmann ME, Huang H, Tindall DJ. Androgen receptor signaling in androgen-refractory prostate cancer. J Natl Cancer Inst 2001;93:1687–97.
19. Hobisch A, Culig Z, Radmayr C, Bartsch G, Klocker H, Hittmair A. Distant metastases from prostatic carcinoma express androgen receptor protein. Cancer Res 1995;55:3068–72.
20. Hobisch A, Culig Z, Radmayr C, Bartsch G, Klocker H, Hittmair A. Androgen receptor status of lymph node metastases from prostate cancer. Prostate 1996;28:129–35.
21. Visakorpi T, Hyytinen E, Koivisto P, Tanner M, Keinanen R, Palmberg C, Palotie A, Tammela T, Isola J, Kallioniemi OP. In vivo amplification of the androgen receptor gene and progression of human prostate cancer. Nat Genet 1995;9:401–6.
22. Taplin ME, Bubley GJ, Shuster TD, Frantz ME, Spooner AE, Ogata GK, Keer HN, Balk SP. Mutation of the androgen-receptor gene in metastatic androgen-independent prostate cancer. N Engl J Med 1995; 332:1393–8.
23. van der Kwast TH, Schalken J, Ruizeveld der Winter JA, van Vroonhoven CCJ, Mulder E, Boersma W, Trapman J. Androgen receptors in endocrine-therapy-resistant human prostate cancer. Int J Cancer 1991; 48:189–93.

24. Ruizeveld de Winter JA, Janssen PJ, Sleddens HM, Verleun-Mooijman MC, Trapman J, Brinkmann AO, Santerse AB, Schroder FH, van der Kwast TH. Androgen receptor status in localized and locally progressive hormone refractory human prostate cancer. Am J Pathol 1994;144:735–46.
25. Montironi R, Magi-Galluzzi C, Fabris G. Apoptotic bodies in prostatic intraepithelial neoplasia and prostatic adenocarcinoma following total androgen ablation. Pathol Res Prac 1995;191:873–80.
26. Yang G, Wheeler TM, Kattan MW, Scardino PT, Thompson TC. Perineural invasion of prostate carcinoma cells is associated with reduced apoptotic index. Cancer 1996;78:1267–71.
27. Palmberg C, Rantala I, Tammela TL, Helin H, Koivisto PA. Low apoptotic activity in primary prostate carcinomas without response to hormonal therapy. Oncol Rep 2000;7:1141–4.
28. Krajewska M, Krajewski S, Epstein JI, Shabaik A, Sauvageot J, Song K, Kitada S, Reed JC. Immunohistochemical analysis of bcl-2, bax, bcl-X, and mcl-1 expression in prostate cancers. Am J Pathol 1996; 148:1567–76.
29. Raffo AJ, Perlman H, Chen MW, Day ML, Streitman JS, Buttyan R. Overexpression of bcl-2 protects prostate cancer cells from apoptosis in vitro and confers resistance to androgen depletion in vivo. Cancer Res 1995;55:4438–45.
30. McConkey DJ, Greene G, Pettaway CA. Apoptosis resistance increases with metastatic potential in cells of the human LNCaP prostate carcinoma line. Cancer Res 1996;56:5594–9.
31. McDonnell TJ, Troncoso P, Brisbay SM, Logothetis C, Chung LW, Hsieh JT, Tu SM, Campbell ML. Expression of the protooncogene bcl-2 in the prostate and its association with emergence of androgen-independent prostate cancer. Cancer Res 1992;52:6940–4.
32. Navone NM, Troncoso P, Pisters LL, Goodrow TL, Palmer JL, Nichols WW, von Eschenbach AC, Conti CJ. p53 protein accumulation and gene mutation in the progression of human prostate carcinoma. J Natl Cancer Inst 1993;85:1657–69.
33. Heidenberg HB, Sesterhenn IA, Gaddipati JP, Weghorst CM, Buzard GS, Moul JW, Srivastava S. Alteration of the tumor suppressor gene p53 in a high fraction of hormone refractory prostate cancer. J Urol 1995;154:414–21.
34. Myers RB, Oelschlager D, Srivastava S, Grizzle WE. Accumulation of the p53 protein occurs more frequently in metastatic than in localized prostatic adenocarcinomas. Prostate 1994;25:243–8.
35. Apakama I, Robinson MC, Walter NM, Charlton RG, Royds JA, Fuller CE, Neal DE, Hamdy FC. bcl-2 overexpression combined with p53 protein accumulation correlates with hormone-refractory prostate cancer. Br J Cancer 1996;74:1258–62.
36. Bauer JJ, Sesterhenn IA, Mostofi FK, McLeod DG, Srivastava S, Moul JW. Elevated levels of apoptosis regulator proteins p53 and bcl-2 are independent prognostic biomarkers in surgically treated clinically localized prostate cancer. J Urol 1996;156:1511–6.
37. Israels LG, Israels ED. Apoptosis. Oncologist 1999;4:332–9.
38. Sordello S, Bertrand N, Plouet J. Vascular endothelial growth factor is up-regulated in vitro and in vivo by androgens. Biochem Biophys Res Commun 1998;251:287–90.
39. Stewart RJ, Panigrahy D, Flynn E, Folkman J. Vascular endothelial growth factor expression and tumor angiogenesis are regulated by androgens in hormone responsive human prostate carcinoma: evidence for androgen dependent destabilization of vascular endothelial growth factor transcripts. J Urol 2001;165:688–93.
40. Mazzucchelli R, Montironi R, Santinelli A, Lucarini G, Pugnaloni A, Biagini G. Vascular endothelial growth factor expression and capillary architecture in high-grade PIN and prostate cancer in untreated and androgen-ablated patients. Prostate 2000;45:72–9.
41. Jain RK, Safabakhsh N, Sckell A, Chen Y, Jiang P, Benjamin L, Yuan F, Keshet E. Endothelial cell death, angiogenesis, and microvascular function after castration in an androgen-dependent tumor: role of vascular endothelial growth factor. Proc Natl Acad Sci USA 1998; 95:10820–5.

[CANCER RESEARCH 63, 2206–2215, May 1, 2003]

Constitutive Activation of Nuclear Factor κB p50/p65 and Fra-1 and JunD Is Essential for Deregulated Interleukin 6 Expression in Prostate Cancer[1]

Luiz F. Zerbini, Yihong Wang, Je-Yoel Cho, and Towia A Libermann[2]

BIDMC Genomics Center and New England Baptist Bone and Joint Institute, Beth Israel Deaconess Medical Center and Harvard Medical School, Boston, Massachusetts 02115

ABSTRACT

To date, no effective treatment for patients with advanced androgen-independent prostate cancer is available, whereas androgen ablation therapy, surgery, and radiation therapy are effective in treating local, androgen-dependent tumors. The mechanisms underlying the differences between androgen-dependent and -independent prostate cancer remain elusive. Interleukin (IL)-6 is a pleiotropic cytokine whose expression under normal physiological conditions is tightly controlled. However, aberrant constitutive IL-6 gene expression has been implicated in prostate cancer progression and resistance to chemotherapy and has been directly linked to prostate cancer morbidity and mortality. Particularly striking is the large increase in the expression of IL-6 in hormone-refractory prostate cancer. IL-6, in addition to its role as an immunomodulatory cytokine, functions as a growth and differentiation factor for prostate cancer cells. To determine the molecular mechanisms that lead to deregulated IL-6 expression in advanced prostate cancer, we examined the regulatory elements involved in IL-6 gene expression in androgen-independent prostate cancer cells. We demonstrate that, in contrast to the androgen-sensitive LNCaP cells, androgen-insensitive PC-3 and DU145 cells express high levels of IL-6 protein and mRNA due to enhanced promoter activity. Deregulated activation of the IL-6 promoter is for the most part mediated by a combined constitutive activation of the nuclear factor (NF)-κB p50 and p65 and the activator protein 1 (AP-1) JunD and Fra-1 family members as demonstrated by electrophoretic mobility shift assays, site-directed mutagenesis, and transfection experiments. Mutation of the NF-κB and AP-1 sites drastically reduces IL-6 promoter activity in both androgen-independent prostate cancer cell lines. Additionally, inhibition of these transcription factors using adenovirus vectors encoding either the IκBα repressor gene or a dominant negative JunD mutant leads to a strong down-regulation of IL-6 gene expression at the mRNA and protein level as measured by real-time PCR and ELISA, respectively. Furthermore, the blockade of IL-6 gene expression results in drastic inhibition of the constitutively activated signal transducers and activators of transcription 3 signaling pathway in DU145 cells. Our data demonstrate for the first time that a combined aberrant activation of NF-κB p50 and p65 and AP-1 JunD and Fra-1 in androgen-independent prostate cancer cells results in deregulated IL-6 expression, suggesting a novel potential entry point for therapeutic intervention in prostate cancer.

INTRODUCTION

Prostate cancer has become the most common solid cancer in older men and is one of the most frequent causes of cancer deaths. Although local prostate cancer is slow-growing and many times asymptomatic, advanced prostate cancer, upon conversion from an initially androgen-dependent state into an androgen-independent state, becomes resilient to any known therapy and invariably results in death of the patient. The lack of effective therapies reflects in part the lack of knowledge about the molecular mechanisms involved in the development, progression, and metastasis of this disease. Especially little is known about how androgen-dependent prostate cancer gets converted into androgen-independent, highly metastatic prostate cancer.

IL-6[3] is a pleiotropic cytokine with a wide range of immune and hematopoietic activities. IL-6 expression is tightly regulated and can be induced in macrophages, synovial fibroblasts, endothelial cells, and other cell types. IL-6 plays a crucial role in autoimmune diseases because abnormally high quantities of IL-6 are found in several autoimmune diseases (1). The majority of agents that induce IL-6 gene expression are inflammatory agents including cytokines such as IL-1, TNF-α, and IFN-γ; bacterial endotoxins such as LPS; and viruses (1). High levels of IL-6 have also been observed in a variety of human cancers such as prostate cancer, renal cancer, and multiple myeloma, raising the possibility that IL-6 may play a critical role in cancer development or progression (2–5). The importance of IL-6 for multiple myeloma growth has been established, and interference with IL-6 function is being exploited in clinical trials as a treatment for multiple myeloma.

Serum levels of IL-6 are significantly elevated in patients with hormone-refractory prostate cancer, and IL-6 has been suggested to be a mediator of morbidity and mortality in patients with metastatic disease (2, 3, 5, 6). Prostate cancer cells themselves are constitutively secreting a major portion of IL-6, although other sources such as stromal cells cannot be excluded. Because prostate cancer cells also express high levels of IL-6 receptor, IL-6 may elicit both paracrine and autocrine responses. Androgen-sensitive prostate cancer cell lines such as LNCaP do not express IL-6, but androgen-independent prostate cancer cell lines such as PC-3 and DU145 do express IL-6 (Ref. 2 and this report). However, LNCaP cells can be induced to express IL-6 by treatment with the cytokine IL-1β (7). This distinction between androgen-sensitive and androgen-insensitive prostate cancer cell lines is also reflected in their responses to IL-6. Whereas IL-6 induces G_1 growth arrest and neuroendocrine differentiation of hormone-dependent LNCaP cells, IL-6 is an important growth factor for hormone-refractory PC-3 cells (2, 8).

Thus, prostate cancer cells may convert from a hormone-dependent IL-6-inhibited state into a hormone-refractory IL-6-dependent state. Elevated IL-6 levels in prostate cancer patients correlate with increased serum PSA levels (9). Indeed, IL-6 up-regulates AR activity in DU145 cells transfected with an AR expression vector in a ligand-independent manner and induces AR-dependent PSA gene expression in LNCaP cells in the absence of androgen (10). The exact mechanism of IL-6-mediated AR activation is not clear, but it appears to involve direct interaction of the IL-6 receptor with the ErbB2 and ErbB3 receptors, leading to tyrosine phosphorylation of ErbB2 and ErbB3 and stimulation of protein kinase A and mitogen-activated protein kinase signaling pathways (11).

Received 10/3/02; accepted 2/25/03.

The costs of publication of this article were defrayed in part by the payment of page charges. This article must therefore be hereby marked *advertisement* in accordance with 18 U.S.C. Section 1734 solely to indicate this fact.

[1] Supported by NIH Grant 1RO1 CA85467 and United States Army Medical Research Center Grant DAMD17-01-1-0023 (to T. A. L.).

[2] To whom requests for reprints should be addressed, at BIDMC Genomics Center and New England Baptist Bone and Joint Institute, Beth Israel Deaconess Medical Center and Harvard Medical School, Harvard Institutes of Medicine, 4 Blackfan Circle, Boston, MA 02115. Phone: (617) 667-3393; Fax: (617) 975-5299; E-mail: tliberma@bidmc.harvard.edu.

[3] The abbreviations used are: IL, interleukin; NF, nuclear factor; AP-1, activator protein 1; STAT, signal transducers and activators of transcription; TNF, tumor necrosis factor; LPS, lipopolysaccharide; PSA, prostate-specific antigen; AR, androgen receptor; JAK, Janus kinase; PME, primary mammary epithelial; PREC, primary prostate epithelial cell; CAT, chloramphenicol acetyltransferase; β-gal, β-galactosidase; EMSA, electrophoretic mobility shift assay; ChIP, chromatin immunoprecipitation; hIL, human interleukin; MOI, multiplicity of infection; RT-PCR, reverse transcription-PCR; GAPDH, glyceraldehyde-3-phosphate dehydrogenase; hGAPDH, human glyceraldehyde-3-phosphate dehydrogenase; MRE, multiple response element.

1-min interval at the maximum setting to generate 400-bp to 1-kb DNA fragments, followed by centrifugation for 10 min at 14,000 × *g* at 4°C. Supernatants were collected, and 100 μl of chromatin preparation were aliquoted as the input fraction. The remainder of the supernatants was diluted in buffer [1% Triton X-100, 2 mM EDTA, 150 mM NaCl, 20 mM Tris-HCl, 1× protease inhibitor mixture (pH 7.9)], followed by immunoclearing with 2 μg of sheared salmon sperm DNA, 20 μl of normal rabbit serum, and protein A-Sepharose [45 μl of 50% slurry in 10 mM Tris-HCl (pH 8.1), 1 mM EDTA (Amersham Pharmacia Biotech)] for 2 h at 4°C. Immunoprecipitation was performed overnight at 4°C with 0.5 μg of specific antibody, anti-NF-κB p65 (Santa Cruz Technologies), or normal rabbit serum as a negative control. After immunoprecipitation, 45 μl of protein A-Sepharose and 2 μg of sheared salmon sperm DNA were added, and the incubation was continued for another 1 h. Precipitates were washed sequentially for 10 min each in TSE I [0.1% SDS, 1% Triton X-100, 2 mM EDTA, 20 mM Tris-HCl (pH 8.0), 150 mM NaCl), TSE II (0.1% SDS, 1% Triton X-100, 2 mM EDTA, 20 mM Tris-HCl (pH 8.0), 500 mM NaCl], and TSE III [0.25 M LiCl, 1% NP40, 1% deoxycholate, 1 mM EDTA, 10 mM Tris-HCl (pH 8.0)]. Precipitates were then washed three times with $T_{10}E_1$ buffer (pH 8.0) and extracted three times with 1% SDS, 0.1 M $NaHCO_3$. Eluates were pooled and heated at 65°C overnight to reverse the formaldehyde cross-linking. DNA fragments were purified with the QIAquick PCR purification kit (Qiagen). IL-6 promoter-specific PCR was performed using 2 μl of a 50-μl DNA extraction in Tris EDTA buffer with Hi-Fi Taq polymerase (Invitrogen). PCR mixtures were amplified for 1 cycle at 94°C for 2 min; followed by 32 cycles at 94°C for 30 s, annealing temperature of 55°C for 30 s, and 68°C for 1 min; and then subjected to a final elongation at 68°C for 5 min. The primers used, hIL6P-F3 (5′-GCTAGCCT-CAATGACGACCT-3′) and hIL6P-R3 (5′-GCCTCAGACATCTCCAGTCC-3′), amplify 222 bp of the hIL-6 promoter surrounding the NF-κB site.

Adenovirus Construction and Infection. The adenovirus encoding the IκB gene was kindly provided by Fionula Brennan (24). The adenovirus encoding dominant negative JunD and the β-gal gene were generated using the ADENO-X system from Clontech Laboratories, Inc. The dominant negative JunD mutant was obtained from the pCMV5-JundΔ plasmid, kindly provided by Dr. Lester F. Lau, University of Illinois (25). The fragment encoding the β-gal gene was from pCMVβ plasmid (Clontech Laboratories, Inc.). Briefly, the dominant negative JunD mutant cDNA was inserted into appropriate restriction sites inside the polylinker of the pShuttle vector (3.9 kb), creating an independent expression cassette. The cassette was transferred to pAdeno-X (32.6 kb) containing adenoviral DNA by means of an *in vitro* ligation at the sole restriction sites *I-Ceu*I and *PI-Sce*I. The ligation was digested by *Swa*I to linearize nonrecombinant (self-ligated) pAdeno-X DNA. The cosmids were then used to transform DH5α electrocompetent bacterial cells, using standard molecular biology techniques. Because pShuttle and pAdeno-X carry different antibiotic selection markers, purification of the expression cassette fragment before ligation was not required. The recovered ampicillin-resistant clones were screened by PCR analysis and restriction endonuclease digestion. Clones containing the desired construct were amplified, and large scale DNA purification was performed. The recombinant adenovirus vectors were then linearized by digestion with *Pac*I to correctly expose the two inverted terminal repeats, thus allowing adenovirus replication and bacterial plasmid sequence excision. The DNAs were transfected in HEK 293 cells using LipofectAMINE Plus reagent (Life Technologies, Inc.). Cytopathic effects were evident 10–12 days after transfection. When most of the cells were detached, the suspension was collected, and the viruses were isolated using freeze/thaw cycles (−20°C/37°C). The expression of the transgenes is under the control of the strong human cytomegalovirus immediate early promoter/enhancer ($P_{CMV\ IE}$) and the polyadenylation signal from the bovine growth hormone gene. For virus purification, HEK 293 cells were plated on a large scale (approximately 30 plates, 150-cm^2 dishes, 80% confluent) and infected with the recombinant adenovirus obtained after transfection. Following the cytopathic effect, cells were collected in a centrifuge tube (15 ml) and centrifuged at 6000 × *g* for 20 min, and the supernatant was discarded. The cell pellet was then resuspended in PBS, submitted to five freeze/thaw cycles, and centrifuged at 6000 × *g* for 10 min. The supernatant was recovered, and the virus was purified by two steps of CsCl gradient (26). The virus band was recovered and dialyzed against 10 mM Tris (pH 7.4), 1 mM $MgCl_2$, 10% glycerol solution. Determination of virus particle titer was accomplished spectrophotometrically by the method described by Maizel *et al.* (27) with a conversion factor of 1.1×10^{12} viral particles per unit at 260 nm. To determine the titer of infectious viral particles on HEK 293 cells, a plaque assay was used as described by Mittereder *et al.* (26). The infection experiments were carried out in serum-free medium during 1 h at 37°C with a MOI of 1000.

IL-6 ELISA. DU145 and PC-3 cells at 10^6 cells/ml were infected with Ad5IκB, Ad5-DNJunD, or both together using Ad5-β-gal as a negative control for 24, 48, and 72 h. IL-6 in the supernatant was assayed by ELISA (BioSource International Inc., Camarillo, CA) using a monoclonal antibody specific for hIL-6 according to the protocol supplied by the manufacturer.

RT-PCR Analysis. Total RNA was harvested using QIAshreder (Qiagen) and RNeasy Mini Kit (Qiagen). cDNA was generated from 2 μg of total RNA using Ready-to-Go You-Prime First-Strand Beads (Amersham Pharmacia Biotech). RT-PCR amplifications of 0.1 μg of cDNA were carried out using a MJ Research thermal cycler PTC-100 as follows: 5 min at 94°C; 35 cycles of 30 s at 94°C, 45 s at 50°C, and 1 min at 72°C; followed by 5 min at 72°C. The sequences of the IL-6 primers were 5′-GGGAACGAAAGAGAAGCTCT-3′ (sense) and 5′-ACCAGAAGAAGGAATGCCCA-3′ (antisense), with an expected size of 730 bp. The sequences of the primers for hGAPDH were 5′-CAAAGTTGTCATGGATGACC-3′ (sense) and 5′-CCATGGAGAAG-GCTGGGG-3′ (antisense), with an expected size of 195 bp.

Real-Time PCR. Total RNA and cDNA were generated as described in RT-PCR analysis. SYBR Green I-based real-time PCR was carried out on a MJ Research DNA Engine Opticon Continuous Fluorescence Detection System (MJ Research Inc., Walthan, MA). All PCR mixtures contained PCR buffer [final concentration, 10 mM Tris-HCl (pH 9.0), 50 mM KCl, 2 mM $MgCl_2$, and 0.1% Triton X-100], 250 μM deoxynucleoside triphosphate (Roche Molecular Biochemicals), 0.5 μM of each PCR primer, 0.5× SYBR Green I (Molecular Probes), 5% DMSO, and 1 unit of Taq DNA polymerase (Promega, Madison, WI) with 2 μl of cDNA in a 25-μl final volume reaction mix. The samples were loaded into wells of Low Profile 96-well microplates. After an initial denaturation step for 1 min at 94°C, conditions for cycling were 35 cycles of 30 s at 94°C, 30 s at 50°C, and 1 min at 72°C. The fluorescence signal was measured right after incubation for 5 s at 75°C following the extension step, which eliminates possible primer dimer detection. At the end of the PCR cycles, a melting curve was generated to identify specificity of the PCR product. For each run, serial dilutions of hGAPDH plasmids were used as standards for quantitative measurement of the amount of amplified DNA. For normalization of each sample, hGAPDH primers were used to measure the amount of hGAPDH cDNA. All samples were run in triplicates, and the data were presented as ratio of IL-6:GAPDH and then as a percentage of β-gal control sample or LNCaP cells control sample. The primers used for real-time PCR are described in RT-PCR analysis.

Western Blot Analysis. Whole cell lysates were prepared in lysis buffer [20 mM Tris (pH 7.4), 150 mM NaCl, 1 mM EDTA, 1 mM EGTA, 1% Triton X-100, 2.5 mM Na PP_i, 1 mM β-glycerolphosphate, 1 mM Na_3VO_4, 1 μg/ml leupeptin, and 1 mM phenylmethylsulfonyl fluoride]. Thirty μg of protein were electrophoresed in a 10% acrylamide-SDS gel. Proteins were electroblotted onto a polyvinylidene difluoride membrane in a 50 mM Tris-base, 20% methanol, 40 mM glycine electrophoresis buffer. Membranes were incubated in 5% nonfat dry milk in TBST (60 mM Tris-base, 120 mM NaCl, and 0.2% Tween 20) for 1 h. Blots were probed with anti-STAT3 antibody (Cell Signaling) or anti-phospho-STAT3 antibody (Cell Signaling) overnight at 4°C in 2% BSA in TBST and then incubated with a horseradish peroxidase-conjugated secondary antibody (Cell Signaling) in 5% dry milk in TBST for 1 h at room temperature. Bound antibodies were detected by chemiluminescence with ECL detection reagents (Amersham Pharmacia Biotech) and visualized by autoradiography.

RESULTS

Androgen-independent Prostate Cancer Cell Lines Constitutively Express IL-6. Highly elevated constitutive expression of IL-6 has been observed in advanced prostate cancer as well as a variety of other cancers. To establish a prostate cancer model system in which to study deregulated IL-6 gene expression, we tested a variety of prostate cancer cell lines as well as PRECs for endogenous IL-6 gene expression by RT-PCR (Fig. 2). At the same time, we also evaluated breast cancer cell lines and primary mammary gland epithelial cells for IL-6

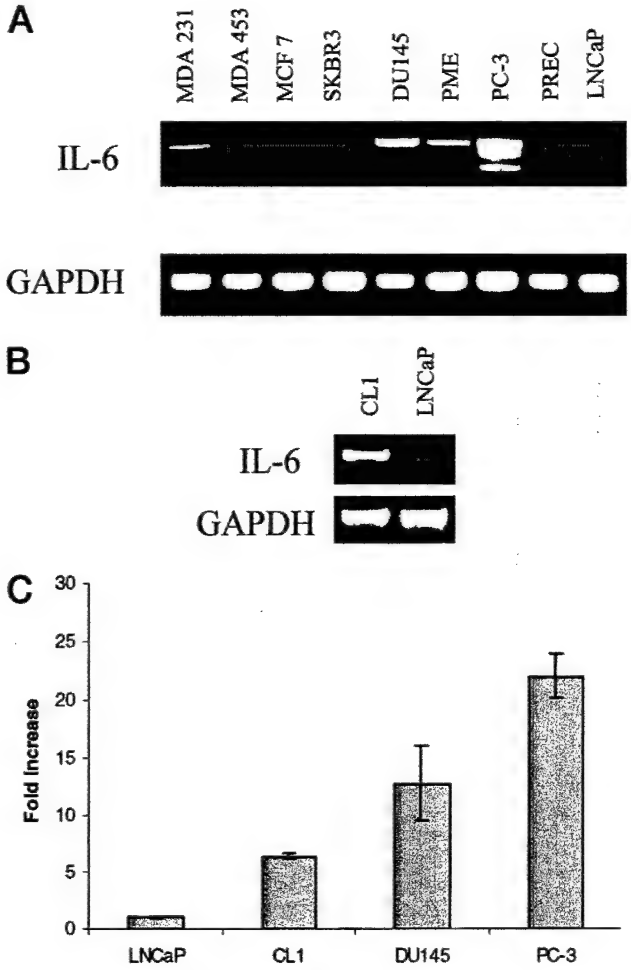

Fig. 2. Expression of IL-6 mRNA in prostate and breast cancer cell lines. mRNA was analyzed by RT-PCR and real-time PCR using IL-6- and GAPDH-specific primers as described in "Materials and Methods." *A*, total RNA isolated from DU145, PC-3, and LNCaP prostate cancer cells; MDA231, MDA435, MCF7, and SKBR3 breast cancer cells; PME cells; and PRECs was analyzed by RT-PCR using IL-6- and GAPDH-specific primers as described in "Materials and Methods." *B*, total RNA isolated from CL1 and LNCaP prostate cancer cells was analyzed by RT-PCR using IL-6- and GAPDH-specific primers as described in "Materials and Methods." *C*, total RNA isolated from PC-3, DU145, CL1, and LNCaP prostate cancer cells was analyzed by real-time PCR. The reactions were carried out in triplicates using the SYBR Green I methodology and primers specific for hGAPDH and hIL-6. Normalization of each sample was carried out by measuring the amount of hGAPDH cDNA. Data were presented as fold increase over the LNCaP cell control sample.

expression (Fig. 2*A*). As reported previously, androgen-independent PC-3 and DU145 prostate cancer cells expressed high levels of IL-6 mRNA. PC-3 cells expressed significantly higher levels of IL-6 than DU145 cells. In contrast to the androgen-insensitive prostate cancer cells, androgen-sensitive LNCaP prostate cancer cells were devoid of IL-6 mRNA (Fig. 2*A*). Multiple PCR products were observed in PC-3 cells, most likely indicating the expression of alternatively spliced transcripts of the IL-6 gene because the IL-6 PCR primers used in this experiment anneal in the 5′-untranslated region and 3′-untranslated region, respectively. It has been demonstrated previously that the hIL-6 gene can transcribe at least six different alternatively spliced transcripts (28). Low levels of IL-6 mRNA were also detected in PRECs and mammary gland epithelial cells that represent relatively undifferentiated, proliferating epithelial cells of the prostate and mammary gland, respectively (Fig. 2*A*). Of the four breast cancer cell lines examined (MDA231, MDA453, MCF7, and SKBR3), only MDA231 cells expressed IL-6 (Fig. 2*A*).

Although DU145 and PC-3 cells have been used in many studies as models for advanced, androgen-independent prostate cancer, both cell lines do not exactly reflect advanced, hormone-refractory prostate cancer *in vivo*. In contrast to DU145 and PC-3 cells, hormone-refractory prostate cancer cells do express PSA and AR and preferentially metastasize to the bone. To confirm that deregulated IL-6 expression in DU145 and PC-3 cells can be used as a model system for studying IL-6 expression and indeed reflects some aspects of the conversion of androgen-dependent to androgen-independent prostate cancer, we evaluated IL-6 expression in a clonal cell line, CL1, generated upon conversion of the androgen-sensitive LNCaP cells to an androgen-insensitive state by the removal of androgen in the media. As described previously, the LNCaP cells were devoid of IL-6 mRNA (Fig. 2*B*). However, CL1 cells showed high levels of IL-6 expression, similar to the DU145 and PC-3 cells (Fig. 2*B*). These data provide direct evidence that androgen-sensitive prostate cancer cells start to express IL-6 upon loss of androgen dependence. To quantify the amount of IL-6 mRNA present in the cells, we tested LNCaP, CL1, DU145, and PC-3 prostate cancer cell lines for endogenous IL-6 gene expression by real-time PCR (Fig. 2). Androgen-independent PC-3, DU145, and CL1 prostate cancer cells expressed 22, 12.8, and 6.4 times higher levels of IL-6 mRNA than androgen-sensitive LNCaP cells, further supporting the data obtained by RT-PCR (Fig. 2*C*). Due to the low transfection efficiency in CL1 cells, we decided to use the DU145 and PC-3 cells to further define the molecular mechanisms of IL-6 gene expression in prostate cancer cells.

IL-6 Expression in Prostate Cancer Cell Lines Correlates with IL-6 Promoter Activity. To determine whether constitutive IL-6 expression in prostate cancer cells is due to enhanced transcription of the IL-6 promoter, we assessed whether endogenous IL-6 expression correlates with IL-6 promoter activity. The full-length human 1.2-kb IL-6 promoter was inserted into the pxp2 reporter gene construct containing the luciferase gene and transiently transfected into the PC-3, DU145, and LNCaP prostate cancer cell lines. Transfection of pxp2-IL6 resulted in a 2000-, 270-, and 6-fold transcriptional stimulation of the IL-6 promoter construct as compared with the parental pxp2 vector in PC-3, DU145, and LNCaP cells, respectively (Fig. 3). These data demonstrate that constitutive expression of IL-6 in prostate cancer cells directly correlates with its promoter activity and that PC-3 cells express the highest IL-6 promoter activity.

Deregulated IL-6 Gene Expression in Prostate Cancer Cells Is Predominantly a Result of Constitutive NF-κB p50/p65 and AP-1 Fra-1/JunD Activation. To determine which regulatory elements in the IL-6 promoter mediate deregulated IL-6 gene expression in prostate cancer cells, the wild-type IL-6 promoter CAT construct and IL-6 promoter constructs with point mutations in either the NF-κB, AP-1, MRE, or NF-IL-6 binding sites were transiently transfected into PC-3 and DU145 cells. Mutations of either the NF-κB or AP-1 site reduced IL-6 promoter activity in both cell lines drastically but not completely, indicating that NF-κB and AP-1 are constitutively active in androgen-independent prostate cancer cells and are critical transcription factors for IL-6 gene expression in prostate cancer cells (Fig. 4). A less pronounced reduction in IL-6 promoter activity was observed in PC-3 cells, but not in DU145 cells, when the MRE was mutated, whereas the NF-IL-6 element appears not to play any role in prostate cancer cells (Fig. 4). Similar experiments were carried out using plasmids containing combined mutations in both the NF-κB and AP-1 binding sites. Combined NF-κB/AP-1 mutation within the context of the IL-6 promoter did not significantly enhance the decrease in IL-6 promoter activity when compared with single mutations in either the NF-κB or AP-1 site, suggesting cooperativity between NF-κB and AP-1 (data not shown). Thus, mutation of either site appears to affect activity of the other site. In an effort to confirm that NF-κB binds to the IL-6 promoter *in vivo*, we performed a ChIP assay in PC-3 human prostate

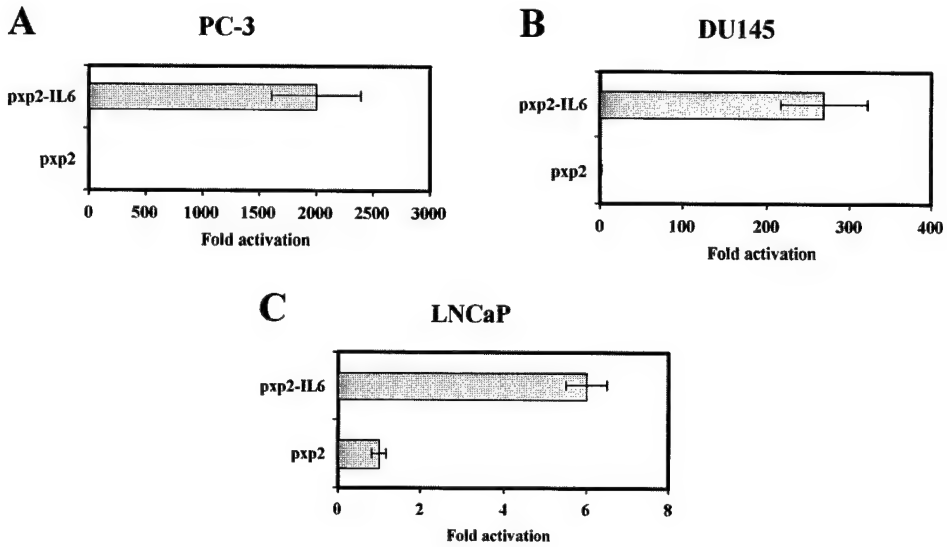

Fig. 3. Transcriptional activity of the IL-6 promoter in DU145, PC-3, and LNCaP prostate cancer cell lines. The cells were transfected with either the full-length IL-6 promoter luciferase construct (pXP2-IL6) or the parental vector (pXP2). Luciferase activity in the lysates was determined 16 h later, as described. Data shown are means ± SDs of duplicates of one representative transfection and normalized by measuring the amount of β-gal gene expression. The experiment was repeated three times with different plasmid preparations with comparable results. The luciferase activity of the IL-6 promoter is shown as fold induction of the parental vector as indicated on the *left*. *A*, androgen-independent PC-3 cells; *B*, androgen-independent DU145 cells; *C*, androgen-sensitive LNCaP cells.

cancer cells. Immunoprecipitation of the cross-linked protein-DNA complexes with an antibody against NF-κB p65 was followed by analysis of the immunoprecipitated DNA by PCR using IL-6 promoter-specific primers spanning −220 to +2 surrounding the NF-κB site of the hIL-6 promoter. As shown in Fig. 4*C*, immunoprecipitation of chromatin with anti-NF-κB p65 antibody, but not control normal rabbit serum, specifically enriched for the endogenous IL-6 promoter DNA, demonstrating that NF-κB p65 binds *in vivo* to the IL-6 promoter in PC-3 cells.

NF-κB is a ubiquitous transcription factor that is activated by a variety of proinflammatory cytokines, bacterial endotoxins, viral infection, DNA damage, and free radicals. In unstimulated cells under normal physiological conditions, NF-κB is maintained in the cytoplasm as an inactive complex with members of the IκB inhibitor family (29–33). This interaction inhibits nuclear translocation and the DNA binding activity of NF-κB. Cellular stimulation leads to phosphorylation, ubiquitination, and subsequent proteolysis of IκB in proteasomes, enabling NF-κB to translocate into the nucleus and to activate a variety of genes including cytokines, cell cycle-regulatory genes, and antiapoptotic genes.

To evaluate whether prostate cancer cells that express IL-6 differ in their NF-κB activity from prostate cancer cells that do not express IL-6, we performed EMSAs using whole cell extracts from IL-6-expressing PC-3 and DU145 cells and non-IL-6-expressing LNCaP cells. Our EMSA data clearly demonstrated that NF-κB is constitutively activated in PC-3 and DU145 cells, but not in LNCaP cells (Fig. 5*A*), directly correlating with IL-6 expression and promoter activity. A strong protein-DNA complex comigrated with the NF-κB complex formed in IL-1-stimulated U-138 MG human glioma cells. To further delineate which members of the NF-κB/rel family are activated in prostate cancer cells, we performed a supershift assay with antibodies against different members of the NF-κB/rel family. These experiments established that the NF-κB family members p50 and p65 make up the constitutively active NF-κB complex in both PC-3 and DU145 cells (Fig. 5*B*), whereas c-rel, p52, and rel B are not involved (Fig. 5*C*). Previous experiments with NF-κB elements in other promoters and cell extracts from other types of cells had demonstrated that all antibodies are able to shift the specific family member in nuclear extracts (data not shown). Additional EMSA analysis using cell extracts from DU145 and PC-3 cells overexpressing the IκB inhibitor gene demonstrated that IκB overexpression abolished NF-κB binding in PC-3 and DU145 cells (data not shown).

AP-1 has been implicated in a variety of biological processes including cell differentiation, proliferation, apoptosis, and oncogenic transformation. AP-1 activity is modulated both by enhanced expression and by interactions with other transcriptional regulators and is further controlled by upstream kinases that link AP-1 to various signal transduction pathways (34–36). AP-1 proteins contain basic region leucine zipper domains and act as a variety of homo- or heterodimers composed of members of the Fos, Jun, and ATF families (2, 37–39). Whereas the Fos proteins can only heterodimerize with members of the Jun family, the Jun proteins can both homo-dimerize and heterodimerize with Fos members to form transcription active complexes (2, 18, 40).

Similarly to NF-κB, EMSA analysis demonstrated constitutive activation of AP-1 in IL-6-positive PC-3 and DU145 cells and the lack of AP-1 in IL-6-negative LNCaP cells (Fig. 5), further enhancing the notion that constitutive activation of IL-6 gene expression in prostate cancer cells is due to constitutive activation of NF-κB and AP-1. Surprisingly, supershift analysis using antibodies recognizing various members of the Jun and Fos families identified JunD and Fra-1 as the predominant proteins present in the complex (Fig. 5, *D* and *E*). These results clearly demonstrate that deregulated IL-6 gene expression in prostate cancer cells is for the most part mediated by constitutive activation of NF-κB p50 and p65 and AP-1 JunD and Fra-1.

Inhibition of NF-κB and AP-1 Strongly Down-Regulates IL-6 Gene Expression and IL-6 Protein Secretion in Androgen-independent Prostate Cancer Cells. Having demonstrated that NF-κB and AP-1 play major roles in deregulated IL-6 promoter activity in prostate cancer, we went on to determine whether interference with NF-κB and/or AP-1 activity would down-regulate IL-6 expression in androgen-independent prostate cancer cells. Previous experiments have shown that overexpression of the IκB inhibitor blocks NF-κB activity. Inhibition of NF-κB by the superrepressor form of IκB has also been shown to block the antiapoptotic activity of NF-κB, thereby facilitating apoptosis through a variety of therapeutic agents and TNF-α (29, 32, 33, 41, 42). To determine the importance of the NF-κB and AP-1 binding sites for endogenous IL-6 gene expression in prostate cancer cells, we infected androgen-independent PC-3 and DU145 prostate cancer cells with an adenovirus encoding the IκB gene (Ad5CMVIκB), an adenovirus encoding the dominant negative mutant JunD gene (AD5CMV-DNJunD), or both adenoviruses together (Ad5CMVIκB/Ad5CMVDNJunD), or an adenovirus carrying the β-gal gene (Ad5CMVβ-gal) as a control at a MOI of 1000. Total

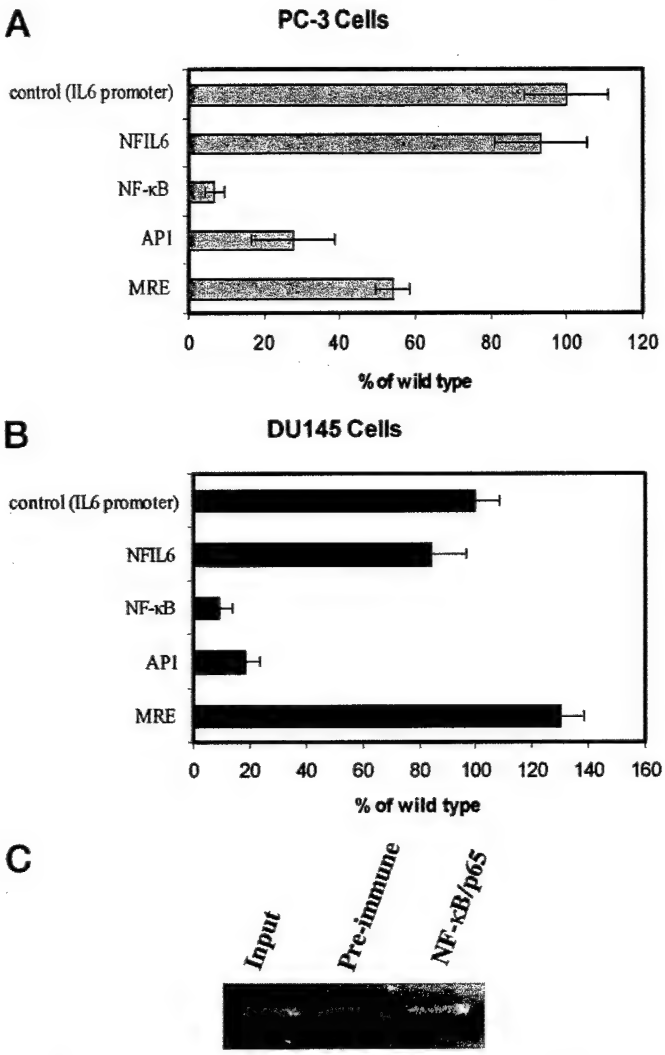

Fig. 4. AP-1 and NF-κB elements are the predominant elements for IL-6 promoter activity in androgen-insensitive prostate cancer cells. *A* and *B*, site-directed mutations within the AP-1 and NF-κB elements diminish IL-6 promoter activity in androgen-independent prostate cancer cells. PC-3 (*A*) and DU145 (*B*) cells were transiently transfected with either the full-length IL-6 promoter CAT construct (pIL6-CAT) or the IL-6 promoter-CAT construct in which the specified *cis*-regulatory element had been eliminated by site-directed mutagenesis. The CAT activity in the lysates was determined 16 h later, as described above. Data shown are means ± SDs of duplicates of one representative transfection. The experiment was repeated three times with different plasmid preparations with comparable results. The CAT activity of the IL-6 promoter is shown as the percentage of induction of the wild-type IL-6 promoter as indicated on the *left*. *C*, anti-NF-κB p65 antibody specifically enriches IL-6 promoter DNA sequences in a ChIP assay. Chromatin proteins were cross-linked to DNA in PC-3 cells by formaldehyde, and purified nucleoprotein complexes were immunoprecipitated using either Anti-NF-κB p65 antibody (*Lane 3*) or nonspecific rabbit IgG (*Lane 2*). The precipitated DNA fractions were analyzed by PCR for the presence of the IL-6 promoter region. In each case, the input DNA (1:100 dilution) was used as a positive control (*Lane 1*). Amplification products were analyzed on a 2% agarose gel and visualized by ethidium bromide staining.

RNA and tissue culture supernatant were obtained from cells infected with Ad5CMVIκB, Ad5CMVDNJunD, Ad5CMVIκB/Ad5CMVDNJunD, or Ad5CMVβ-gal at 24, 48, and 72 h after infection. Real-time PCR revealed that overexpression of IκB and dominant negative JunD led to a strong down-regulation of IL-6 gene expression in both cell lines that was sustained for at least 72 h (Fig. 6), further supporting the notion that the NF-κB and AP-1 binding sites are crucial for activation of the IL-6 gene in prostate cancer cells. Ad5CMVIκB infection reduced IL-6 mRNA expression down to 43.2%, 53.2%, and 65.4% of the control for the different time points in DU145 cells and down to 46.6%, 59.6%, and 58.7% of the control for the different time points in PC-3 cells (Fig. 6). Overexpressing the dominant negative JunD mutants reduced the levels of IL-6 gene expression down to 48.8%, 34.2%, and 52.1% of the control in DU145 cells and down to 43.3%, 39.9%, and 66.3% of the control in PC-3 cells. Combined infection with both adenoviruses resulted in an additive effect on IL-6 down-regulation. In this case, IL-6 gene expression was down to 25.7%, 24.1%, and 37.7% of the control in DU145

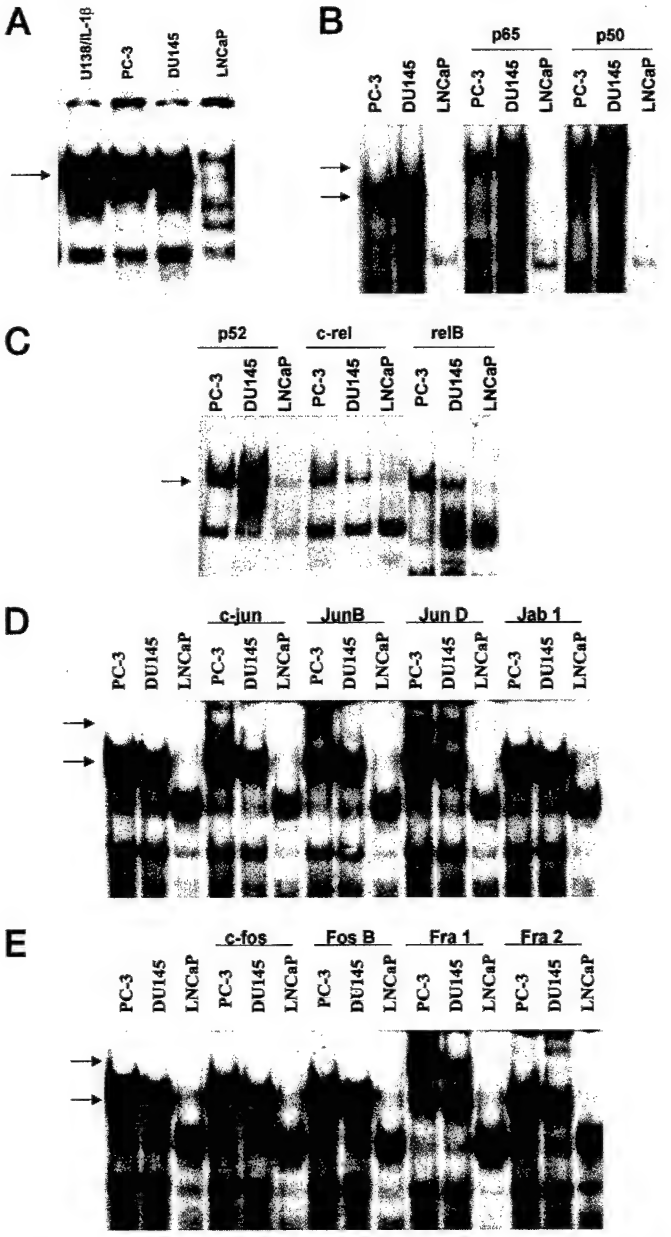

Fig. 5. EMSA of prostate cancer cell extracts for the IL-6 promoter NF-κB and AP-1 elements. Five μg of DU145, PC-3, and LNCaP whole cell lysates were incubated with ^{32}P-labeled oligonucleotides encoding the IL-6 promoter NF-κB and AP-1 sites, and DNA-protein complexes were visualized on nondenaturing polyacrylamide gels. *A*, interaction of the IL-6 promoter NF-κB binding site with prostate cancer cell lysates. Extracts of U-138 MG cells treated with IL-1β were used as a positive control for activated NF-κB. The *arrow* indicates the specific DNA-protein complex. *B* and *C*, supershift assay for NF-κB/rel family members. The DU145, PC-3, and LNCaP whole cell extracts were incubated with the labeled IL-6/NF-κB oligonucleotide probe in the absence or presence of antibodies against p50, p65, p52, c-rel, and relB. The *arrows* indicate the NF-κB DNA-protein complex and the supershifted antibody-protein-DNA complex. *D*, interaction of the IL-6 promoter AP-1 binding site with prostate cancer cell extracts and supershift assay for AP-1 family members. The DU145, PC-3, and LNCaP whole cell extracts were incubated with the labeled IL-6/AP-1 oligonucleotide probe with either no antibody or antibodies against c-jun, JunB, JunD, and JAB1. *E*, supershifts with antibodies against c-fos, FosB, Fra-1, and Fra-2. The *arrows* indicate the AP-1 DNA-protein complex protein and the supershifted antibody-protein-DNA complex.

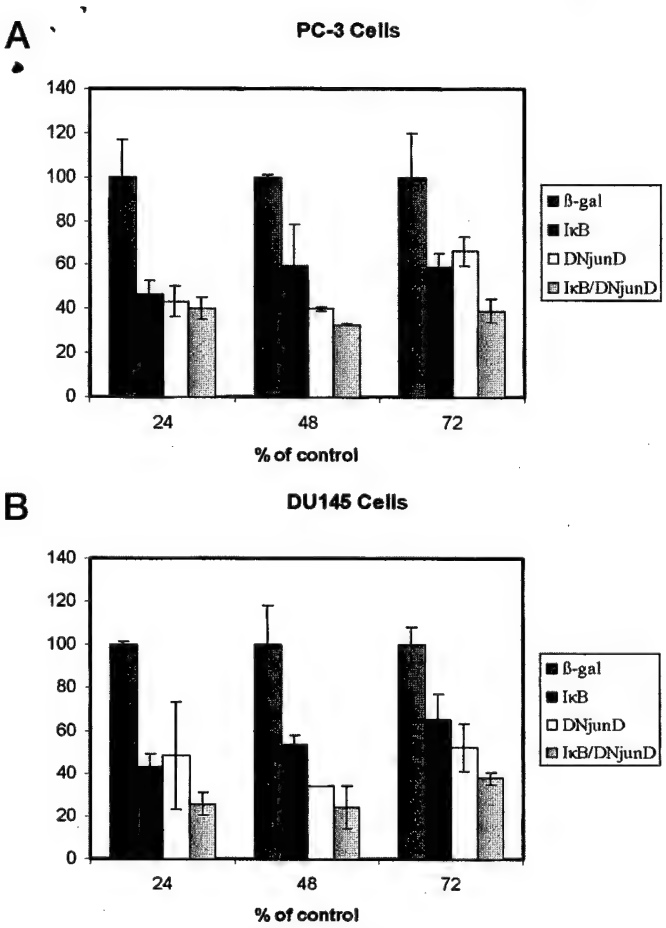

Fig. 6. Blockage of NF-κB and AP-1 activity down-regulates IL-6 gene expression in androgen-independent prostate cancer cells. DU145 and PC-3 cells were infected with an adenovirus expressing IκB, an adenovirus encoding dominant negative JunD, or both adenoviruses together, using an adenovirus expressing the β-gal gene as a control at a MOI of 1000. Total RNA was isolated at 24, 48, and 72 h after infection. Real-time PCR reactions were carried out in triplicates using the SYBR Green I methodology and primers specific for hGAPDH and hIL-6. Normalization of each sample was carried out by measuring the amount of hGAPDH cDNA. Data were presented as fold increase over the β-galactosidase control sample.

cells and 40.2%, 32.9%, and 39.2% of the control in PC-3 cells. However, the total expression of IL-6 mRNA molecules in DU145 cells was approximately three time less than that in PC-3 cells after infection with the viruses (data not shown). Because IL-6 expression was not completely blocked, it is possible that additional transcription factors play roles in IL-6 expression in prostate cancer cells.

Protein expression and mRNA expression do not necessarily correlate. To determine whether the blockage of NF-κB and AP-1 and the subsequent reduction in IL-6 mRNA levels have an effect on IL-6 protein secretion, we analyzed IL-6 protein levels in tissue culture supernatants obtained from DU145 and PC-3 cells infected with the same virus combination as described above at 24, 48, and 72 h. IL-6-specific ELISA analysis revealed that overexpression of IκB and dominant negative JunD leads to drastic inhibition of IL-6 protein secretion in both cell lines (Fig. 7). IκB overexpression showed a 3.8-, 4.0-, and 2.7-fold inhibition of IL-6 secretion in DU145 cells and a 1.8-, 2.9-, and 3.9-fold inhibition of IL-6 in PC-3. Dominant negative JunD overexpression resulted in a 2.0-, 1.31-, and 1.73-fold inhibition of IL-6 secretion in DU145 and a 4.3-, 4.2-, and 2.2-fold inhibition of IL-6 secretion in PC-3 cells. The highest fold inhibition was obtained when the cell lines were infected with both viruses together (Fig. 7). In DU145 cells, the simultaneous blockage of NF-κB and AP-1 showed a 12.5-, 11-, and 8.23-fold inhibition of IL-6 protein levels in comparison with the control at 24, 48, and 72 h, respectively. The same experiment in PC-3 revealed a 5.4-, 8.5-, and 7.4-fold inhibition of IL-6 secretion. These data corroborate the IL-6 mRNA expression experiments and most vividly show the importance of constitutively activated NF-κB and AP-1 for deregulated IL-6 gene expression in prostate cancer cells.

Inhibition of IL-6 Secretion and Gene Expression by IκB Overexpression Blocks the Autocrine, STAT3-activating Trigger by IL-6. IL-6 utilizes JAK-STAT as major mediators of signal transduction (16, 17, 43). To further delineate the effect of inhibition of IL-6 gene expression and IL-6 secretion due to overexpression of IκB gene on the autocrine activity of IL-6, we tested the activity of STAT3, one of the signal transducers of IL-6, in PC-3 and DU145 cells by immunoblotting with an anti-phospho-Tyr^{705} antibody specific for the tyrosine-phosphorylated active form of STAT3 in a time course experiment. We observed that down-regulation of IL-6 gene expression blocks STAT3 phosphorylation efficiently at 48 and 72 h in DU145 cells, correlating with the reduction in IL-6 levels at those time points. In contrast to DU145 cells, PC-3 cells expressed only very low levels of STAT3 protein and had no STAT3 activity (Fig. 8).

DISCUSSION

Although androgen ablation therapy, surgery, and radiation therapy are effective for the treatment of local prostate cancer, there is no effective treatment available for patients with the metastatic andro-

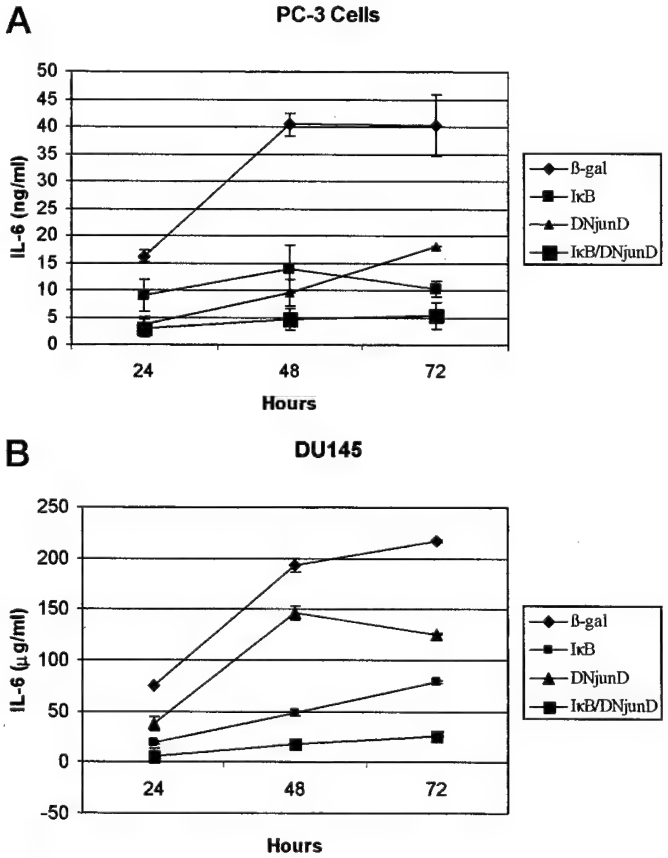

Fig. 7. Overexpression of the IκB repressor and dominant negative JunD inhibits IL-6 secretion in DU145 and PC-3 androgen-independent prostate cancer cells. DU145 and PC-3 cells were infected with an adenovirus expressing IκB, an adenovirus expressing dominant negative JunD, or both adenoviruses together, using an adenovirus encoding β-galactosidase gene as a control. The immunoreactivity in the cell supernatant was determined by an IL-6-specific ELISA at 24, 48, and 72 h after infection. *A*, IL-6 ELISA measurement in PC-3 cells; *B*, IL-6 ELISA measurement in DU145 cells.

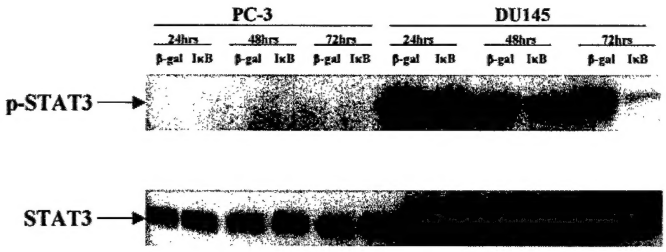

Fig. 8. Overexpression of the IκB repressor blocks constitutive activation of STAT3 in DU145 prostate cancer cells. PC-3 and DU145 cells were infected with either an adenovirus expressing IκB or an adenovirus encoding the β-galactosidase gene as a control. The total cell lysate was collected at 24, 48, and 72 h after infection. The extracts were then subjected to immunoblot analysis using antibodies against either tyrosine-phosphorylated active STAT3 (Tyr^{705}) or total STAT3.

gen-independent disease. The poor prognosis for androgen-independent advanced prostate cancer reflects in part the lack of knowledge about the tumor's basic biology. A variety of differences between androgen-sensitive and androgen-insensitive prostate cancer have been revealed over the last few years. However, despite that accumulation of additional and new data about these differences, the crucial steps that lead to progression and conversion of androgen-dependent to androgen-independent, metastatic prostate cancer remain elusive. One feature of advanced prostate cancer that particularly triggered our interest is the sudden deregulated activation of the IL-6 gene in advanced, androgen-independent prostate cancer, but not in primary, androgen-dependent prostate cancer. Furthermore, the level of IL-6 found in prostate cancer patients directly correlates with morbidity and mortality of the patients, further enhancing the notion that the IL-6 gene may be a key to understanding and treating advanced prostate cancer.

Deregulated IL-6 expression has been implicated in a variety of other cancers, particularly in multiple myeloma, where it is clear that IL-6 is a major growth factor for cancer cells and a major target for potential therapies. In addition to its potential growth and differentiation effects in prostate cancer, IL-6 is also antiapoptotic and interferes with chemotherapies. IL-6 could also affect neighboring prostate tumor cells by a paracrine mechanism that could affect prostate tumor cell invasion as well as growth (44). Nevertheless, the importance of IL-6 *per se* for prostate cancer progression is not entirely clear, and it is possible that IL-6 is only one of several genes that act in a similar fashion in synergy but are regulated by the same upstream signals. Therefore, IL-6 may represent a surrogate marker for prostate cancer progression, but interference with IL-6 as a therapeutic modality may not work because IL-6 is only one of several factors with a similar function. We therefore argued that understanding the regulation of IL-6 gene expression in prostate cancer may elucidate the upstream factors that deregulate expression of a whole set of genes involved in advanced prostate cancer. These upstream factors should be far more desirable points of interference for novel therapies than IL-6 itself.

Although IL-6 expression in advanced prostate cancer has been previously observed, very little attention has been focused until now on the mechanism of this deregulated IL-6 expression. We confirm here that indeed only androgen-insensitive prostate cancer cell lines such as LNCaP-derived CL1 cells and PC-3 and DU145 cells, but not androgen-sensitive prostate cancer cell lines such as LNCaP, constitutively express IL-6. This result is consistent with previous reports and enables us to use these prostate cancer cell lines as a cell culture model for the study of aberrant IL-6 gene expression (2, 3, 5, 45). As a first step to delineate the molecular mechanisms leading to deregulated IL-6 gene expression in advanced prostate cancer we defined the transcription factors that constitutively activate the IL-6 gene in androgen-independent prostate cancer. We now demonstrate that deregulated IL-6 expression in prostate cancer cells directly correlates with IL-6 promoter activity, although changes in RNA stability or protein secretion may also play some role. This result immediately suggests that activation of IL-6 expression upon progression from an androgen-sensitive, IL-6-negative prostate cancer to a hormone-refractory, IL-6-positive prostate cancer is for the most part due to constitutive activation of a transcription factor or transcription factors that turn on the IL-6 gene and/or constitutive repression of a transcriptional suppressor of the IL-6 gene. Systematic analysis of IL-6 promoter activity in hormone-refractory prostate cancer cell lines enabled us to identify two regulatory elements, NF-κB and AP-1, whose activity correlates with IL-6 expression in prostate cancer cells and is essential for constitutive IL-6 gene expression in prostate cancer cells. Point mutations in the NF-κB and AP-1 binding sites drastically reduced IL-6 promoter activation in androgen-independent prostate cancer cell lines, although there was some residual promoter activity left, leaving the possibility open that additional regulatory elements may be involved. We identified the members of the NF-κB and AP-1 family that are constitutively active in hormone-refractory prostate cancer cells as the NF-κB heterodimer of p50 and p65 and the AP-1 heterodimer of JunD and Fra-1, and we demonstrated that p65 binds *in vivo* to the IL-6 promoter.

Although the activation of NF-κB in prostate cancer cell lines has been observed previously, no direct link between constitutive activation of NF-κB and IL-6 had been demonstrated up to now. The blockage of NF-κB activity in human prostate cancer cells has been associated with invasion and metastasis (46) and enhanced TNF-α-induced apoptosis (47, 48), and our results indicate that one of the mechanisms may involve the inhibition of IL-6 expression. Similarly, AP-1 activation in prostate cancer cell lines has been reported, and it has been suggested that NF-κB and AP-1 may play a role in the survival of prostate cancer cells (42, 47, 49–51). However, the particular members of the NF-κB and AP-1 family that are active in prostate cancer cells had not been identified until now. Indeed, this is the first report indicating activation of JunD and Fra-1 in advanced prostate cancer cells, although sporadic activation of these factors in some other cancer types has been reported. Furthermore, our results are the first evidence that activated JunD and Fra-1 play a critical role in IL-6 gene expression in prostate cancer cells. Similarly to p50 and p65, JunD and Fra-1 form heterodimers that act as activating transcription factors on a variety of target genes. Strikingly, blocking either NF-κB or JunD drastically inhibits IL-6 expression and secretion as well as the downstream signaling pathways such as activation of STAT3 in prostate cancer cells, and a combination of both inhibitors further enhances this blockade. This inhibition is most likely direct inhibition of IL-6 promoter activation but could also involve indirect mechanisms of action via other genes regulated by NF-κB or AP-1 that affect IL-6 expression. However, in contrast to DU145 cells, PC-3 cells express only very low levels of STAT3, suggesting that IL-6 in PC-3 cells acts via a different mechanism that may include other members of the STAT family such as STAT1. Activation of STAT3 has been shown to enhance growth of prostate cancer cells (52, 53) and neuroendocrine differentiation (54), and constitutive STAT3 activation has been observed in prostate cancer, indicating that blocking STAT3 activation due to inhibition of IL-6 expression via AP-1 and NF-κB may be beneficial. Thus, we envision that a rational drug design with the purpose to intervene efficiently with advanced prostate cancer should target both NF-κB and JunD/Fra-1 concomitantly. To prove this hypothesis, we are now determining whether targeting AP-1 and NF-κB will interfere with prostate cancer growth and survival. Indeed, both AP-1 and NF-κB have been implicated in growth and survival in many different cell types (55–58), although there is significantly less known about the JunD and Fra-1

AP-1 family members than about p50 and p65. To further our understanding of the role of AP-1 and NF-κB in prostate cancer, we are in the process of evaluating the functional consequences of AP-1 and NF-κB activation in prostate cancer.

AP-1 and NF-κB are targets for a variety of different external stimuli that elicit their biological responses via a wide array of signal transduction pathways. Activators of AP-1 and NF-κB include, among others, various cytokines, growth factors, tumor promoter 12-*O*-tetradecanoylphorbol-13-acetate, reactive oxygen species, bacterial endotoxin LPS, viral infection, and UV light (59–71). The specific trigger leading to constitutive activation of AP-1 and NF-κB in prostate cancer is not yet known, but it may include the constitutive activation of a cytokine or growth factor that activates AP-1 and NF-κB via an autocrine mechanism. To elucidate this mechanism is an important goal of our current efforts, and this upstream regulator of AP-1 and NF-κB may turn out to be a master switch for prostate cancer progression.

It does not come as a surprise that both AP-1 and NF-κB are activated in prostate cancer because AP-1 and NF-κB have been implicated in the pathogenesis of a variety of human cancers, and several cancer types have been reported to concomitantly activate AP-1 and NF-κB (43, 72–76). For example, transformed keratinocytes contain constitutively active AP-1 and NF-κB, and both are required for maintaining the transformed phenotype. Similarly, AP-1 and NF-κB are activated in pancreatic cancer and head and neck squamous cell carcinoma cell lines (14, 59, 75, 77, 78). Furthermore, a variety of genes involved in cancer are regulated by the combined action of AP-1 and NF-κB such as IL-6, IL-8, MMP-9, COX-2, and MCP-1, suggesting that AP-1 and NF-κB cooperate synergistically in regulating a wide array of genes. However, in contrast to prostate cancer cells, in most cases the activated AP-1 complex contains c-jun and c-fos rather than Fra-1 and JunD.

In conclusion, our results have elucidated some of the major transcriptional regulatory mechanisms leading to deregulated IL-6 expression in advanced prostate cancer and have proven that blockage of these regulatory mechanisms can inhibit IL-6 expression and signal transduction in prostate cancer. Because IL-6 and possibly other genes with similar functions may be regulated by the same set of transcription factors, namely, AP-1 and NF-κB, combined interference with these transcription factors may give rise to novel therapeutic modalities in the fight against prostate cancer.

ACKNOWLEDGMENTS

We acknowledge fruitful discussions with Drs. Ellen Gravallese, Xuesong Gu, Franck Grall, Gina Napoleone, Jon Jones, Mehmet Inan, Rosana Kapeller-Libermann, and Glen Bubley.

REFERENCES

1. Hirano, T. The biology of interleukin-6. Chem. Immunol., *51:* 153–180, 1992.
2. Chung, T. D., Yu, J. J., Spiotto, M. T., Bartkowski, M., and Simons, J. W. Characterization of the role of IL-6 in the progression of prostate cancer. Prostate, *38:* 199–207, 1999.
3. Drachenberg, D. E., Elgamal, A. A., Rowbotham, R., Peterson, M., and Murphy, G. P. Circulating levels of interleukin-6 in patients with hormone refractory prostate cancer. Prostate, *41:* 127–133, 1999.
4. Hirano, T., Akira, S., Taga, T., and Kishimoto, T. Biological and clinical aspects of interleukin 6. Immunol. Today, *11:* 443–449, 1990.
5. Okamoto, M., Lee, C., and Oyasu, R. Interleukin-6 as a paracrine and autocrine growth factor in human prostatic carcinoma cells *in vitro*. Cancer Res., *57:* 141–146, 1997.
6. Twillie, D. A., Eisenberger, M. A., Carducci, M. A., Hseih, W. S., Kim, W. Y., and Simons, J. W. Interleukin-6: a candidate mediator of human prostate cancer morbidity. Urology, *45:* 542–549, 1995.
7. Maliner-Stratton, M. S., Klein, R. D., Udavakumar, T. S., Nagle, R. B., and Bowden, G. T. Interleukin-1β-induced promatrilysin expression is mediated by NFκB-regulated synthesis of interleukin-6 in the prostate carcinoma cell line, LNCaP. Neoplasia, *3:* 509–520, 2001.
8. Mori, S., Murakami-Mori, K., and Bonavida, B. Interleukin-6 induces G_1 arrest through induction of p27(Kip1), a cyclin-dependent kinase inhibitor, and neuron-like morphology in LNCaP prostate tumor cells. Biochem. Biophys. Res. Commun., *257:* 609–614, 1999.
9. Adler, H. L., McCurdy, M. A., Kattan, M. W., Timme, T. L., Scardino, P. T., and Thompson, T. C. Elevated levels of circulating interleukin-6 and transforming growth factor-β1 in patients with metastatic prostatic carcinoma. J. Urol., *161:* 182–187, 1999.
10. Hobisch, A., Eder, I. E., Putz, T., Horninger, W., Bartsch, G., Klocker, H., and Culig, Z. Interleukin-6 regulates prostate-specific protein expression in prostate carcinoma cells by activation of the androgen receptor. Cancer Res., *58:* 4640–4645, 1998.
11. Qiu, Y., Ravi, L., and Kung, H. J. Requirement of ErbB2 for signalling by interleukin-6 in prostate carcinoma cells. Nature (Lond.), *393:* 83–85, 1998.
12. Borsellino, N., Belldegrun, A., and Bonavida, B. Endogenous interleukin 6 is a resistance factor for *cis*-diamminedichloroplatinum and etoposide-mediated cytotoxicity of human prostate carcinoma cell lines. Cancer Res., *55:* 4633–4639, 1995.
13. Heinrich, P. C., Behrmann, I., Muller-Newen, G., Schaper, F., and Graeve, L. Interleukin-6-type cytokine signalling through the gp130/Jak/STAT pathway. Biochem. J., *334:* 297–314, 1998.
14. Yoon, J. K., and Lau, L. F. Involvement of JunD in transcriptional activation of the orphan receptor gene nur77 by nerve growth factor and membrane depolarization in PC12 cells. Mol. Cell. Biol., *14:* 7731–7743, 1994.
15. Imada, K., and Leonard, W. J. The Jak-STAT pathway. Mol. Immunol., *37:* 1–11, 2000.
16. Lutticken, C., Wegenka, U. M., Yuan, J., Buschmann, J., Schindler, C., Ziemiecki, A., Harpur, A. G., Wilks, A. F., Yasukawa, K., Taga, T., *et al.* Association of transcription factor APRF and protein kinase Jak1 with the interleukin-6 signal transducer gp130. Science (Wash. DC), *263:* 89–92, 1994.
17. Zhong, Z., Wen, Z., and Darnell, J. E., Jr. Stat3: a STAT family member activated by tyrosine phosphorylation in response to epidermal growth factor and interleukin-6. Science (Wash. DC), *264:* 95–98, 1994.
18. Dendorfer, U., Oettgen, P., and Libermann, T. A. Multiple regulatory elements in the interleukin-6 gene mediate induction by prostaglandins, cyclic AMP, and lipopolysaccharide. Mol. Cell. Biol., *14:* 4443–4454, 1994.
19. Libermann, T. A., and Baltimore, D. Activation of interleukin-6 gene expression through the NF-κB transcription factor. Mol. Cell. Biol., *10:* 2327–3234, 1990.
20. Dendorfer, U., Oettgen, P., and Libermann, T. A. Interleukin-6 gene expression by prostaglandins and cyclic AMP mediated by multiple regulatory elements. Am. J. Ther., *2:* 660–665, 1995.
21. Oettgen, P., Carter, K. C., Augustus, M., Barcinski, M., Boltax, J., Kunsch, C., and Libermann, T. A. The novel epithelial-specific Ets transcription factor gene ESX maps to human chromosome 1q32.1. Genomics, *45:* 456–457, 1997.
22. Akbarali, Y., Oettgen, P., Boltax, J., and Libermann, T. A. ELF-1 interacts with and transactivates the IgH enhancer π site. J. Biol. Chem., *271:* 26007–26012, 1996.
23. Oettgen, P., Akbarali, Y., Boltax, J., Best, J., Kunsch, C., and Libermann, T. A. Characterization of NERF, a novel transcription factor related to the Ets factor ELF-1. Mol. Cell. Biol., *16:* 5091–5106, 1996.
24. Bondeson, J., Brennan, F., Foxwell, B., and Feldmann, M. Effective adenoviral transfer of IκBα into human fibroblasts and chondrosarcoma cells reveals that the induction of matrix metalloproteinases and proinflammatory cytokines is nuclear factor-κB dependent. J. Rheumatol., *27:* 2078–2089, 2000.
25. Wolf, J. S., Chen, Z., Dong, G., Sunwoo, J. B., Bancroft, C. C., Capo, D. E., Yeh, N. T., Mukaida, N., and Van Waes, C. IL (interleukin)-1α promotes nuclear factor-κB and AP-1-induced IL-8 expression, cell survival, and proliferation in head and neck squamous cell carcinomas. Clin. Cancer Res., *7:* 1812–1820, 2001.
26. Mittereder, N., March, K. L., and Trapnell, B. C. Evaluation of the concentration and bioactivity of adenovirus vectors for gene therapy. J. Virol., *70:* 7498–7509, 1996.
27. Maizel, J. V., Jr., White, D. O., and Scharff, M. D. The polypeptides of adenovirus. I. Evidence for multiple protein components in the virion and a comparison of types 2, 7A, and 12. Virology, *36:* 115–125, 1968.
28. Bihl, M. P., Heinimann, K., Rudiger, J. J., Eickelberg, O., Prruchoud, A. P., Tamm, M., and Roth, M. Identification of a novel IL-6 isoform binding to the endogenous IL-6 receptor. Am. J. Respir. Cell Mol. Biol., *27:* 48–56, 2002.
29. Baeuerle, P. A., and Baltimore, D. NF-κB: ten years after. Cell, *87:* 13–20, 1996.
30. Karin, M., and Lin, A. NF-κB at the crossroads of life and death. Nat. Immunol., *3:* 221–227, 2002.
31. Miyamoto, S., and Verma, I. M. Rel/NF-κB/IκB story. Adv. Cancer Res., *66:* 255–292, 1995.
32. Van Antwerp, D. J., Martin, S. J., Kafri, T., Green, D. R., and Verma, I. M. Suppression of TNF-α-induced apoptosis by NF-κB. Science (Wash. DC), *274:* 787–789, 1996.
33. Yamasaki, K., Taga, T., Hirata, Y., Yawata, H., Kawanishi, Y., Seed, B., Taniguchi, T., Hirano, T., and Kishimoto, T. Cloning and expression of the human interleukin-6 (BSF-2/IFN β2) receptor. Science (Wash. DC), *241:* 825–828, 1988.
34. Deng, T., and Karin, M. c-Fos transcriptional activity stimulated by H-Ras-activated protein kinase distinct from JNK and ERK. Nature (Lond.), *371:* 171–175, 1994.
35. Han, T. H., and Prywes, R. Regulatory role of MEF2D in serum induction of the c-jun promoter. Mol. Cell. Biol., *15:* 2907–2915, 1995.
36. Hill, C. S., Wynne, J., and Treisman, R. Serum-regulated transcription by serum response factor (SRF): a novel role for the DNA binding domain. EMBO J., *13:* 5421–5432, 1994.
37. Pognonec, P., Boulukos, K. E., Aperlo, C., Fujimoto, M., Ariga, H., Nomoto, A., and Kato, H. Cross-family interaction between the bHLHZip USF and bZip Fra1 proteins results in down-regulation of AP1 activity. Oncogene, *14:* 2091–2098, 1997.

38. van Dam, H., and Castellazzi, M. Distinct roles of Jun:Fos and Jun:ATF dimers in oncogenesis. Oncogene, *20:* 2453–2464, 2001.
39. Vogt, P. K. Jun, the oncoprotein. Oncogene, *20:* 2365–2377, 2001.
40. Chinenov, Y., and Kerppola, T. K. Close encounters of many kinds: Fos-Jun interactions that mediate transcription regulatory specificity. Oncogene, *20:* 2438–2452, 2001.
41. Cheng, J. D., Ryseck, R. P., Attar, R. M., Dambach, D., and Bravo, R. Functional redundancy of the nuclear factor κB inhibitors IκBα and IκBβ. J. Exp. Med., *188:* 1055–1062, 1998.
42. Palayoor, S. T., Youmell, M. Y., Calderwood, S. K., Coleman, C. N., and Price, B. D. Constitutive activation of IκB kinase α and NF-κB in prostate cancer cells is inhibited by ibuprofen. Oncogene, *18:* 7389–7394, 1999.
43. Hsu, T. C., Young, M. R., Cmarik, J., and Colburn, N. H. Activator protein 1 (AP-1)- and nuclear factor κB (NF-κB)-dependent transcriptional events in carcinogenesis. Free Radic. Biol. Med., *28:* 1338–1348, 2000.
44. Stratton, M. S., Sirvent, H., Udayakumar, T. S., Nagle, R. B., and Bowden, G. T. Expression of the matrix metalloproteinase promatrilysin in coculture of prostate carcinoma cell lines. Prostate, *48:* 206–209, 2001.
45. Lou, W., Ni, Z., Dyer, K., Tweardy, D. J., and Gao, A. C. Interleukin-6 induces prostate cancer cell growth accompanied by activation of stat3 signaling pathway. Prostate, *42:* 239–242, 2000.
46. Huang, S., Pettaway, C. A., Uehara, H., Bucana, C. D., and Fidler, I. J. Blockade of NF-κB activity in human prostate cancer cells is associated with suppression of angiogenesis, invasion, and metastasis. Oncogene, *20:* 4188–4197, 2001.
47. Muenchen, H. J., Lin, D. L., Walsh, M. A., Keller, E. T., and Pienta, K. J. Tumor necrosis factor-α-induced apoptosis in prostate cancer cells through inhibition of nuclear factor-κB by an IκBα "super-repressor." Clin. Cancer Res., *6:* 1969–1977, 2000.
48. Wang, C. Y., Mayo, M. W., and Baldwin, A. S., Jr. TNF-α and cancer therapy-induced apoptosis: potentiation by inhibition of NF-κB. Science (Wash. DC), *274:* 784–787, 1996.
49. Chen, C. D., and Sawyers, C. L. NF-κB activates prostate-specific antigen expression and is upregulated in androgen-insensitive prostate cancer. Mol. Cell. Biol., *22:* 2862–2870, 2002.
50. Gupta, S., Afaq, F., and Mukhtar, H. Involvement of nuclear factor-κB, Bax and Bcl-2 in induction of cell cycle arrest and apoptosis by apigenin in human prostate carcinoma cells. Oncogene, *21:* 3727–3738, 2002.
51. Shaulian, E., and Karin, M. AP-1 in cell proliferation and survival. Oncogene, *20:* 2390–2400, 2001.
52. DeMiguel, F., Lee, S. O., Lou, W., Xiao, X., Pflug, B. R., Nelson, J. B., and Gao, A. C. Stat3 enhances the growth of LNCaP human prostate cancer cells in intact and castrated male nude mice. Prostate, *52:* 123–129, 2002.
53. Dhir, R., Ni, Z., Lou, W., DeMiguel, F., Grandis, J. R., and Gao, A. C. Stat3 activation in prostatic carcinomas. Prostate, *51:* 241–246, 2002.
54. Spiotto, M. T., and Chung, T. D. STAT3 mediates IL-6-induced neuroendocrine differentiation in prostate cancer cells. Prostate, *42:* 186–195, 2000.
55. Busuttil, V., Bottero, V., Frelin, C., Imbert, V., Ricci, J. E., Auberger, P., and Peyron, J. F. Blocking NF-κB activation in Jurkat leukemic T cells converts the survival agent and tumor promoter PMA into an apoptotic effector. Oncogene, *21:* 3213–3224, 2002.
56. Fiorini, E., Schmitz, I., Marissen, W. E., Osborn, S. L., Touma, M., Sasada, T., Reche, P. A., Tibaldi, E. V., Hussey, R. E., Kruisbeek, A. M., Reinherz, E. L., and Clayton, L. K. Peptide-induced negative selection of thymocytes activates transcription of an NF-κB inhibitor. Mol. Cell, *9:* 637–648, 2002.
57. Piccioli, P., Porcile, C., Stanzione, S., Bisaglia, M., Bajetto, A., Bonavia, R., Florio, T., and Schettini, G. Inhibition of nuclear factor-κB activation induces apoptosis in cerebellar granule cells. J. Neurosci. Res., *66:* 1064–1073, 2001.
58. Zhang, J., Zhang, D., McQuade, J. S., Behbehani, M., Tsien, J. Z., and Xu, M. c-fos regulates neuronal excitability and survival. Nat. Genet., *30:* 416–420, 2002.
59. Bancroft, C. C., Chen, Z., Yeh, J., Sunwoo, J. B., Yeh, N. T., Jackson, S., Jackson, C., and Van Waes, C. Effects of pharmacologic antagonists of epidermal growth factor receptor, PI3K and MEK signal kinases on NF-κB and AP-1 activation and IL-8 and VEGF expression in human head and neck squamous cell carcinoma lines. Int. J. Cancer, *99:* 538–548, 2002.
60. Bannerman, D. D., Tupper, J. C., Kelly, J. D., Winn, R. K., and Harlan, J. M. The Fas-associated death domain protein suppresses activation of NF-κB by LPS and IL-1β. J. Clin. Investig., *109:* 419–425, 2002.
61. Benderdour, M., Tardif, G., Pelletier, J. P., Di Battista, J. A., Reboul, P., Ranger, P., and Martel-Pelletier, J. Interleukin 17 (IL-17) induces collagenase-3 production in human osteoarthritic chondrocytes via AP-1 dependent activation: differential activation of AP-1members by IL-17 and IL-1β. J. Rheumatol., *29:* 1262–1272, 2002.
62. Bhat-Nakshatri, P., Sweeney, C. J., and Nakshatri, H. Identification of signal transduction pathways involved in constitutive NF-κB activation in breast cancer cells. Oncogene, *21:* 2066–2078, 2002.
63. Fennewald, S. M., Aronson, J. F., Zhang, L., and Herzog, N. K. Alterations in NF-κB and RBP-Jκ by arenavirus infection of macrophages *in vitro* and *in vivo*. J. Virol., *76:* 1154–1162, 2002.
64. Gao, X., Ikuta, K., Tajima, M., and Sairenji, T. 12-*O*-Tetradecanoylphorbol-13-acetate induces Epstein-Barr virus reactivation via NF-κB and AP-1 as regulated by protein kinase C and mitogen-activated TPA protein kinase. Virology, *286:* 91–99, 2001.
65. Guha, M., and Mackman N. LPS induction of gene expression in human monocytes. Cell Signalling, *13:* 85–94, 2001.
66. Kosmidou, I., Vassilakopoulos, T., Xagorari, A., Zakynthinos, S., Papapetropoulos, A., and Roussos, C. Production of interleukin-6 by skeletal myotubes: role of reactive oxygen species. Am. J. Respir. Cell Mol. Biol., *26:* 587–593, 2002.
67. Li, N., and Karin, M. Ionizing radiation and short wavelength UV activate NF-κB through two distinct mechanisms. Proc. Natl. Acad. Sci. USA, *95:* 13012–13017, 1998.
68. Li, T., Dai, W., and Lu, L. Ultraviolet-induced Jun-D activation and apoptosis in myeloblastic leukemia ML-1 cells. J. Biol. Chem., *277:* 32668–32676, 2002.
69. Li, X., Commane, M., Jiang, Z., and Stark, G. R. IL-1-induced NFκB and c-Jun N-terminal kinase (JNK) activation diverge at IL-1 receptor-associated kinase (IRAK). Proc. Natl. Acad. Sci. USA, *98:* 4461–4465, 2001.
70. Ludwig, S., Ehrhardt, C., Neumeier, E. R., Kracht, M., Rapp, U. R., and Pleschka, S. Influenza virus-induced AP-1-dependent gene expression requires activation of the JNK signaling pathway. J. Biol. Chem., *276:* 10990–10998, 2001.
71. Seo, H. J., Park, K. K., Han, S. S., Chung, W. Y., Son, M. W., Kim, W. B., and Surh, Y. J. Inhibitory effects of the standardized extract (DA-9601) of *Artemisia asiatica* Nakai on phorbol ester-induced ornithine decarboxylase activity, papilloma formation, cyclooxygenase-2 expression, inducible nitric oxide synthase expression and nuclear transcription factor κB activation in mouse skin. Int. J. Cancer, *100:* 456–462, 2002.
72. Collins, T. S., Lee, L. F., and Ting, J. P. Paclitaxel up-regulates interleukin-8 synthesis in human lung carcinoma through an NF-κB- and AP-1-dependent mechanism. Cancer Immunol. Immunother., *49:* 78–84, 2000.
73. Harwood, F. G., Kasibhatla, S., Petak, I., Vernes, R., Green, D. R., and Houghton, J. A. Regulation of FasL by NF-κB and AP-1 in Fas-dependent thymineless death of human colon carcinoma cells. J. Biol. Chem., *275:* 10023–10029, 2000.
74. Mitsiades, N., Mitsiades, C. S., Poulaki, V., Chauhan, D., Richardson, P. G., Hideshima, T., Munshi, N., Treon, S. P., and Anderson, K. C. Biologic sequelae of nuclear factor-κB blockade in multiple myeloma: therapeutic applications. Blood, *99:* 4079–4086, 2002.
75. Shi, Q., Le, X., Abbruzzese, J. L., Wang, B., Mujaida, N., Matsushima, K., Huang, S., Xiong, Q., and Xie, K. Cooperation between transcription factor AP-1 and NF-κB in the induction of interleukin-8 in human pancreatic adenocarcinoma cells by hypoxia. J. Interferon Cytokine Res., *19:* 1363–1371, 1999.
76. Sliva, D., English, D., Lyons, D., and Lloyd, F. P., Jr. Protein kinase C induces motility of breast cancers by upregulating secretion of urokinase-type plasminogen activator through activation of AP-1 and NF-κB. Biochem. Biophys. Res. Commun., *290:* 552–557, 2002.
77. Arlt, A., Vorndamm, J., Muerkoster, S., Yu, H., Schmidt, W. E., Folsch, U. R., and Schafer H. Autocrine production of interleukin 1β confers constitutive nuclear factor κB activity and chemoresistance in pancreatic carcinoma cell lines. Cancer Res., *62:* 910–916, 2002.
78. Bancroft, C. C., Chen, Z., Dong, G., Sunwoo, J. B., Yeh, N., Park, C., and Van Waes, C. Coexpression of proangiogenic factors IL-8 and VEGF by human head and neck squamous cell carcinoma involves coactivation by MEK-MAPK and IKK-NF-κB signal pathways. Clin. Cancer Res., *7:* 435–442, 2001.

Another important clinical impact of constitutive IL-6 expression in hormone-refractory prostate cancer is the ability of IL-6 to block TGF-β- and p53-mediated apoptosis. This effect of IL-6 also leads to protection of prostate cancer cells from the cytotoxic effect of chemotherapeutic agents (12). Additionally, the constitutive IL-6 expression activates the JAK-STAT pathway, which has been implicated in multiple cytokine-mediated mechanisms of growth regulation. The JAK-STAT pathway is activated by binding of IL-6 to its receptor complex, consisting of the IL-6 α-receptor subunit and gp130, the β-receptor subunit (13, 14). This event results in autophosphorylation and activation of JAK1, JAK2, and TYK2 (tyrosine kinase 2), leading to recruitment of STAT3, which gets phosphorylated and migrates to the nucleus to activate gene transcription (15–17).

Thus, elevated IL-6 expression in prostate cancer may result in enhanced proliferation of hormone-refractory prostate cancer metastases concomitant with increased drug resistance and inhibition of apoptosis. These results suggest that interference with IL-6 function or expression should be of high clinical relevance in the treatment of hormone-refractory, drug-resistant prostate cancer.

The IL-6 promoter is composed of a variety of overlapping regulatory elements (18, 19). We and others have demonstrated that binding sites for the inducible transcription factors NF-κB, NF-IL-6, cAMP-responsive element binding protein, and AP-1 are essential for induction of the IL-6 gene by LPS, TNF-α, IL-1, phorbol ester, phytohemagglutinin, and double-stranded RNA (18–20). In addition p53, Rb, and glucocorticoid receptors are involved in inhibiting IL-6 gene expression. Although, a variety of regulatory elements are involved in the regulation of IL-6 gene expression, IL-6 promoter regulation in prostate cancer has not yet been explored.

Interference with IL-6 activity could occur either on the level of the protein or by blocking expression of IL-6 mRNA. Because IL-6 may be only one of a set of cytokines and other genes that are aberrantly expressed in prostate cancer with similar activities, blocking the IL-6 protein alone may have only limited success. We propose as an alternative to interfere with the transcription factors involved in constitutive IL-6 gene expression in prostate cancer, with the notion that the same transcription factors regulate a whole set of cytokines and other genes. Thus, blocking one of the critical transcription factors may interfere with transcription of a whole set of cytokines and other genes. Many cytokine promoters contain a similar set of transcription factor binding sites.

In this study, we determined the molecular mechanisms underlying the transcriptional activation of the IL-6 promoter and the deregulated IL-6 gene expression in androgen-independent prostate cancer cells that could provide new tools for therapeutic intervention. We show here that the IL-6 gene is constitutively expressed in two androgen-independent prostate cancer cell lines, PC-3 and DU145. Additionally, the data revealed that endogenous IL-6 gene expression correlates with IL-6 promoter activity and is at least partially mediated via constitutive activation of NF-κB and AP-1. Furthermore, we demonstrated that the blockade of these transcription factors down-regulates IL-6 expression at the mRNA and protein level and leads to inhibition of the phosphorylation of STAT3.

MATERIALS AND METHODS

Cell Culture. The prostate cancer cell lines DU145, PC-3, and LNCaP and the breast cancer cell lines MDA231, MDA435, MCF7, and SKBR3 were obtained from American Type Culture Collection (Manassas, VA). The CL1 prostate cancer cell line was kindly provided by Dr. Sun Paik and Dr. Arie Belldegrun (University of California Los Angeles School of Medicine, Los Angeles, CA). DU145 cells were grown in MEM (Life Technologies, Inc.), PC-3 cells were grown in Ham's F-12 medium (BioWhittaker, Walkersville, MD), LNCaP and CL1 cells were grown in RPMI 1640 (Life Technologies, Inc.), and MDA231, MDA435, MCF7, and SKBR3 cells were grown in DMEM (Life Technologies, Inc.). The media were supplemented with 10% fetal bovine serum (Life Technologies, Inc.) or charcoal-treated serum (CL1), 50 units/ml penicillin, and 50 μg/ml streptomycin (all from Life Technologies, Inc.). PME cells and PRECs were purchased from Clonetics (Walkersville, MD). PME cells were grown in MEGM media (Clonetics), and PRECs were grown in PREGM media (Clonetics). Both media were supplemented with epithelial medium single quote kit, which contains growth factors (Clonetics). The cells were maintained in a 5% CO_2-humidified incubator.

Plasmids. The full-length IL-6 promoter was inserted into the *Bam*HI-*Hin*dIII sites of the pXP2 luciferase vector (pXP2-IL6) as described previously (13). The promoter was also cloned into the pUC-CAT plasmid, generating pIL6-CAT (13), and plasmids carrying point mutations in the MRE, NF-IL-6, AP-1, and NF-κB regulatory elements of the IL-6 promoter (Fig. 1) were generated using site-directed mutagenesis as described previously within the context of the CAT vector (13). The plasmid pβGal-control (BD Biosciences) was used as control for transfection efficiency.

DNA Transfection Assays. Transfections of 3–8 $\times$ 10^5 cells were carried out with 700 ng of reporter gene construct DNA using LipofectAMINE Plus (Life Technologies, Inc.) as described previously (21). The cells were harvested 16 h after transfections and assayed for luciferase activity or CAT enzyme activity. Transfections were performed independently in duplicate and repeated three to four times with different plasmid preparations with similar results. Cotransfection with pβGal-control was used for controlling transfection efficiency. CAT enzyme activity in the transfected cells was determined using the CAT ELISA assay (Roche Molecular Biochemicals, Indianapolis, IN) with a specific antibody to CAT (anti-CAT) according to the protocol supplied by the manufacturer.

EMSA and Supershift Assay. DNA binding reactions and EMSA assays were performed as described previously (22). Whole cell extracts were made from DU145, PC-3, and LNCaP prostate cancer cells using as lysis buffer 1% Triton X-100, 25 mM glycylglycine (pH 7.8), 15 mM $MgSO_4$, 4 mM EGTA, 1 mM DTT, 1 mM phenylmethylsulfonyl fluoride, and 1% aprotinin (Sigma). Protein concentrations were measured by the Bio-Rad protein assay. The reactions were made using 3 μl of whole cell extract and 0.1–0.5 ng of ^{32}P-labeled double-stranded specific oligonucleotides (5,000–25,000 cpm) and run on 4% polyacrylamide gels containing 0.5$\times$ Tris glycine EDTA as described previously (23). For supershift analysis, the cell extracts were preincubated with specific antibodies against different members of the rel/NF-κB family or the AP-1 family (Santa Cruz Technologies) for 20 min before the addition of the labeled probe for an additional 20 min (23). The oligonucleotides used as probes for direct binding studies are as follows: IL-6 promoter wild-type AP-1, 5′-TCGACGTGCTGAGTCACTAAC-3′ and 3′-GCACGACTCAGTGATTGAGCT-5′; and IL-6 promoter wild type NF-κB, 5′-TCGACATGTGGGATTTTCCCATGAC-3′ and 3′-GTACACCCTAAA-AGGGTACTGAGCT-5′.

ChIP. PC-3 human prostate cancer cells (2 $\times$ 10^7) were plated on two 100-mm dishes. Cross-linking was performed by adding formaldehyde directly to tissue culture medium to a final concentration of 1% and incubating for 10 min at room temperature. Cells were rinsed twice with ice-cold PBS and collected into 1 ml of PBS 100 and centrifuged for 5 min at 2,000 $\times$ *g*. Cells were washed sequentially with 1 ml of ice-cold PBS, buffer I [0.25% Triton X-100, 10 mM EDTA, 0.5 mM EGTA, 10 mM HEPES (pH 6.5)] and buffer II [200 mM NaCl, 1 mM EDTA, 0.5 mM EGTA, 10 mM HEPES (pH 6.5)]. Cells were then resuspended in 0.3 ml of lysis buffer [1% SDS, 5 mM EDTA, 50 mM Tris-HCl (pH 8.1), 1$\times$ protease inhibitor mixture (Roche Molecular Biochemicals)], incubated on ice for 10 min, and sonicated three times for 30 s each with

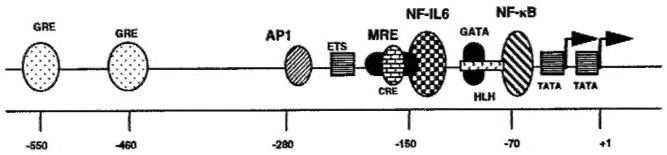

Fig. 1. Regulatory elements of the hIL-6 promoter with their approximate locations relative to the major transcription start site (+1). *GRE*, glucocorticoid response element; *SRE*, serum response element; *CRE*, prostaglandin- and cAMP-responsive element; *HLH*, helix-loop-helix.